Impact tolerant bioinspired materials

Susana M. Estrada H.

Impact tolerant bioinspired materials

A Dissertation

Presented to the School of Engineering

Universidad EAFIT

In partial fulfillment of the requirements for the degree of

Doctor of Philosophy

Engineering

Susana M. Estrada Hernández

April 2020

Abstract

In highly demanding applications, such as sports protective gear and personal body armor, there is a growing demand for lightweight materials able to absorb impact energy while being flexible to allow easy movement to the user. These requirements are generally challenging for typical engineered materials since increased mechanical strength is usually associated with reduced flexibility and increased weight. Fortunately, this dichotomy has been successfully surpassed by natural armor through millions of years of evolution. Through biomimetics, this dissertation sought to introduce the functional principles of segmented natural armor into synthetic devices obtaining a family of cost-efficient materials with enhanced protection and flexibility. Remarkably, these bioinspired materials exhibited a minimum increase of weight enabling its implementation in personal protection applications.

The first Chapter deepens in the main challenges and the prime aims of this work. The second Chapter shows relevant studies related to segmented natural armor, biomimetics, and current bioinspired protection developments. Chapter 3 presents a simplified biomimetic methodology used to introduce the functional principles of segmented natural armor (i.e., segmentation, structural hierarchization, graded mineralization) into synthetic materials. Chapter 4 presents a novel bioinspired mineralization technic to enhance the energy absorption of synthetic materials by mimicking the graded mineralization found in fish scales. Chapter 5 presents a combination of bioinspired ideas to enhance both flexibility and protection generating a family of cost-efficient protecto-flexible materials.

Finally, Chapter 6 presents the main conclusions of this work and some recommendations for future studies.

Content

Figures

Tables

Chapter 1: Introduction

From car-crash events to snake bite attacks, diverse shielding devices have been developed to protect from puncture injuries or impact incidents. Usually, these devices are designed to dissipate the energy associated with dangerous events through the use of tough materials and structures.

1.1 Protection for the human body

When protecting the human body new requirements emerge, since in addition to protection, the shielding devices must provide adequate flexibility and low weight to enable locomotion. For instance, it is usual to find flexible armor in body armor applications known as "soft armor", which is comprised of multiple layers of high-performance flexible fabrics. Soft armor dissipates energy through fiber deformation and inter-fiber friction when fibers slip or slide against each other. This protection strategy allows flexibility but only protects from small projectile impacts. On the contrary, "hard armor" is comprised of rigid panels that can withstand high levels of energy, and for this reason it can protect against high-energy impact events, however, this protection strategy cannot enable flexibility (Hani et al. 2012). Both flexibility and strength are desirable in protective gear where moving parts are involved (e.g., body armor and sports equipment), however, this combination of properties is challenging for typical engineering materials since high strength is usually associated with reduced flexibility. Surprisingly, this extraordinary combination of properties can be found in biological materials and systems, particularly in the segmented dermal armors of some fish, mammals and reptiles (see Figure 1.1).

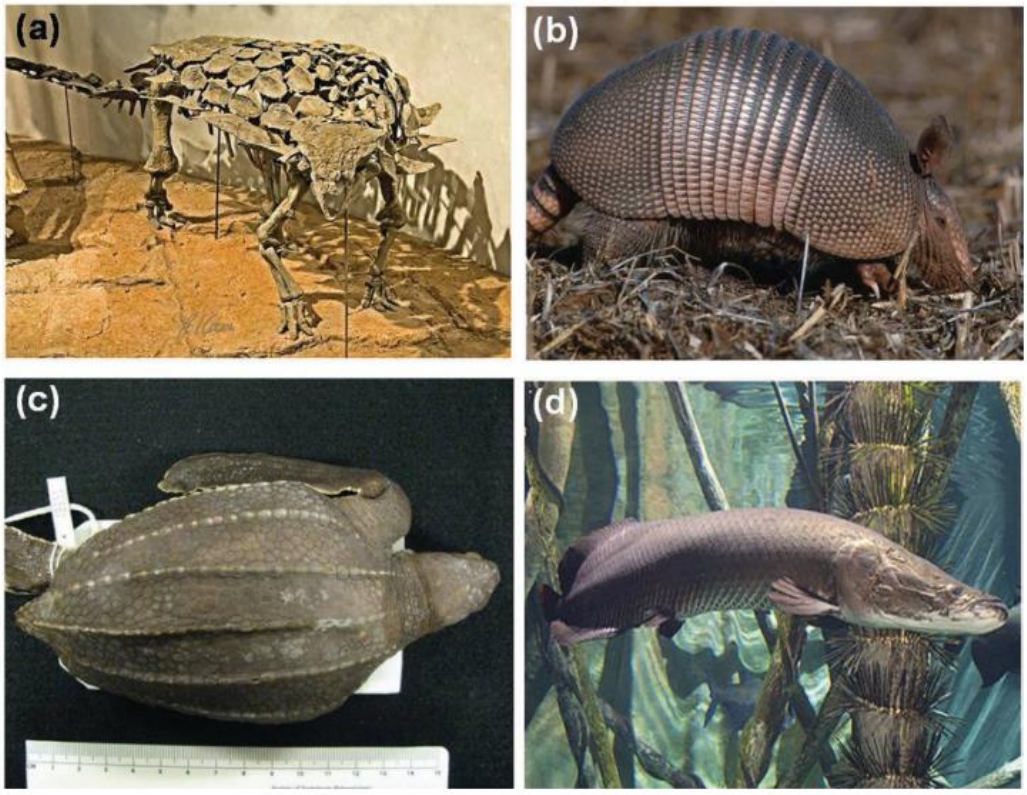

Figure 1.1 Animals with natural flexible dermal armor. (a) dinosaur skeleton, (b) armadillo, (c) leatherback turtle, (d) arapaima. Reproduced from: (Yang, Chen, et al. 2013).

1.2 Biomimetics

Bioinspiration has been used since mythological times as a tool to mimic nature's complex structures. However, the use of bioinspired design methods is still limited for industrial scenarios, since its interdisciplinary nature generates translation challenges between engineers and biologists (Fayemi et al. 2017; M. Helms, Vattam, and Goel 2009; Shu et al. 2011; Wanieck et al. 2016). By presenting a simplified methodology for bioinspired design, this study sought to develop new strategies to guide the use of biomimetics in real development challenges. The simplified methodology presented here consists of a four-step process: 1) Define, 2) Search, 3) Simplify, and 4) Conceptualize.

1.3 Bioinspired flexible protection

By using this methodology to develop flexible protection systems, the armor of some fish, reptiles and mammals were identified as proper biological models. Moreover, the use of the presented biomimetic toolbox allowed to recognize that despite their differences, most of these armors are governed by common functional principles that control their extraordinary performance (i.e., segmentation, structural hierarchization, and graded mineralization).

The identified biological models exhibit a clear similarity: they are covered with hard and stiff units (scales and osteoderms) interconnected together by flexible tissues (skin). In natural designs, these segmented arrangements can achieve high levels of flexibility when compared with monolithic structures, without a significant reduction of strength (Yang, Chen, et al. 2013). To emulate this functional principle, this work proposed to introduce superficial engravings on synthetic protective devices by emulating natural patterns. As in natural analogs, segmentation provided enhanced flexibility to synthetic materials.

Moreover, scales and osteoderms as protective units also share a commonality: they exhibit different distributions of mineral content. Osteoderms on one hand are comprised of dense outer sheaths enclosing a porous core; thus, the difference in porosity causes mineral gradients. On the other hand, the outermost layers of fish's scales present higher degrees of mineral content. Using *Arapaima gigas* fish scales as inspiration, this work proposed to incorporate nano-scale mineral reinforcements into laminar organic fibrous composites. The resulting laminates emulate the graded mineralization present in these

natural structures allowing a considerable enhancement of energy absorption without a significant increase in weight.

Also, as biological tissues, scales and osteoderms are configured in complex hierarchical structures that allow energy dissipation at multiple length scales. These kinds of configurations promote greater armor capability accompanied by a flexible light-weight structure. By introducing structural hierarchization it was able to obtain a family of protecto-flexible materials that increased impact energy absorption while having enhanced flexibility. Further, a bullet-proof protecto-flexible prototype was manufactured and tested, showing that the bioinspired materials can withstand ballistic impacts, and therefore display a promising route to enhance armor systems by using bioinspired methodologies.

The combination of these three functional principles produced biomimetic configurations able to increase up to 251% the combined effect of energy absorption and flexibility on synthetic polymeric materials. Remarkably, these manufacturing strategies allow their implementation into realistic high volumes of production due to their low added costs, so it is envisioned that the proposed biomimetic materials will enable the development of the next generation of high-performance impact-resistant materials.

1.4 Concluding remarks

The search for impact-tolerant, light-weight flexible materials has challenged materials scientists in the last decades. In this quest, many researchers have focused on studying natural armors as a guide to propose bioinspired materials with enhanced properties. Due to its interdisciplinarity, bioinspired design causes translation difficulties between engineers and biologists. Therefore, this doctoral dissertation presents a simplified

methodology for bioinspired design used to develop impact tolerant materials. By extracting the functional principles that underlay the extraordinary performance of segmented natural armor (i.e., segmentation, hierarchization, and graded mineralization), the resulting biomimetic materials exhibited a remarkable combination of properties including light-weight and enhanced protecto-flexibility. Due to the low added costs associated with the fabrication of these biomimetic materials, it is envisioned that they can encourage the development of the next generation of high-performance impact tolerant materials.

Chapter 2: Literature review

The study of natural armor to develop bioinspired flexible protection is not new, on the contrary, many scientists across different disciplines have focused on unraveling the mechanisms that underlay natural protective arrangements aiming to include these concepts in synthetic configurations. To bring order to this dissertation, the current Chapter has been divided into two parts; while the first part describes some of the principles that govern natural flexible armor, the second section shows an overview of biomimetics and how this discipline has been used to develop bioinspired protective systems.

2.1 Segmented natural armor

Natural protection systems range from thin, flexible skins to thick, highly mineralized shells (Dastjerdi, Rabiei, and Barthelat 2013; DiPette, Ural, and Santhanam 2015; Suksangpanya et al. 2017; Zhou et al. 2010). Among hard shells, nacre has received special attention due to its extraordinary toughening mechanisms (F Barthelat and Zhu 2011; Valashani and Barthelat 2015). It is a high-performance natural composite comprised of microscopic mineralized tablets bonded together with a tough biopolymer see Figure 2.1.

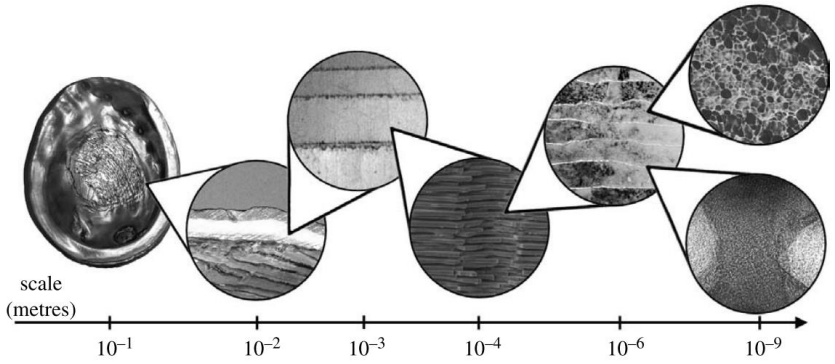

Figure 2.1 Hierarchical structure of Nacre over several length scales. Reproduced from: (Francois Barthelat 2007).

The intermediate solution between soft and hard natural armor is segmented natural armor consisting of hard units (scales or osteoderms) interconnected together with flexible fibers (skin and flexible tissues). This armor alternative is common among a large variety of animal species including fish (Allison et al. 2013; Arola et al. 2018; Lin et al. 2011; M. A. Meyers et al. 2012; Yang et al. 2014; Yang, Gludovatz, et al. 2013; Zimmermann et al. 2013), reptiles (Chen, Yang, and Meyers 2014, 2015; Damiens et al. 2012; C.-Y. Y. Sun and Chen 2013), and mammals (Chen et al. 2011; Liu et al. 2016; Wang et al. 2016). When compared with monolithic configurations, these segmented arrangements provide high levels of flexibility without a significant reduction in strength (Yang, Chen, et al. 2013), and therefore, these configurations have received scientists increasing attention during the last decade.

Fish scales are a good example of segmented natural armor. Scales are light-weight mineralized units arranged in overlapped arrays that enable mobility while providing strong protection from predators. Depending on their structure and composition, fish scales can be classified in four groups: placoid, ganoid, cosmoid and elasmoid, this later group is dived in cycloid and ctenoid (Arola et al. 2018; Bruet et al. 2008; Lin et al. 2011; M. A. Meyers et al. 2012; Sire and Huysseune 2003; Yang et al. 2014; Zimmermann et al. 2013) (Kardong 2012; Martini, Balit, and Barthelat 2017; Murcia et al. 2015). Most scaled systems are found in aquatic animals; however, scales can also offer great defense to Pangolins (i.e., a terrestrial mammal) (Liu et al. 2016; Wang et al. 2016).

Arapaimas and Alligator Gars are freshwater fish cover with scaled systems. Although both animals are large fish that inhabit South and North America basins, their scaled systems present great differences. While Arapaimas are covered with circular elasmoid scales, Gars are protected with rhomboid ganoine scales. Both scale typologies are characterized by presenting higher degrees of mineral content towards the outermost layers of the scale (i.e., graded mineralization). However, their structure differs considerably: while ganoine scales exhibit an external hard layer of ganoine connected to a tough basal bone, elasmoid scales are comprised by unidirectional fiber plies organized in helicoidal arrangements (Allison et al. 2013; Arola et al. 2018; Lin et al. 2011; M. A. Meyers et al. 2012; Murcia et al. 2015; Sherman et al. 2017; Yang et al. 2014; Yang, Gludovatz, et al. 2013; Zimmermann et al. 2013). In bony-based structures such as those found in ganoid scales, the interplay between organic fibrous reinforcements in microscopic mineralized tablets provides extraordinary failure mechanisms that enhance toughness (see Figure 2.2).

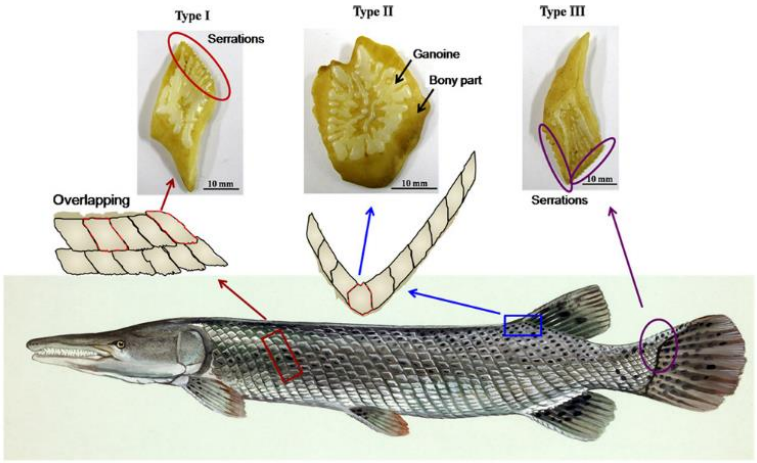

Figure 2.2 Alligator gar: different types of scales located in different parts of the body. Reproduced from: (Yang, Gludovatz, et al. 2013).

On the contrary, the role of fibers and reinforcements in elasmoid scales is the opposite: here the fibrous organic portion is reinforced by minerals (i.e., the matrix) causing unique mechanical effects at different length scales of its hierarchical structure.

Like other biological structural materials, elasmoid scales possess a hierarchical structure (Browning, Ortiz, and Boyce 2013; Khayer Dastjerdi and Barthelat 2015; Vernerey and Barthelat 2010; Yang et al. 2019a; Zhu et al. 2012, 2013). This means that they exhibit a highly organized structure that ranges between the atomic scale to the macro scale (Figure 2.3). They are comprised of a combination of type I collagen fibers and apatite, which are the fundamental constitutive elements among other natural mineralized systems (Yang, Meyers, and Ritchie 2019). Depending on the degree of mineralization, elasmoid scales can be divided into two different layers: a highly mineralized rough external layer termed Limiting Layer (LL), consisting of a mineral matrix with randomly dispersed thin collagen fibers (30 - 50 nm in diameter), and a basal plate commonly regarded as the Elasmodine, which consist of densely packed layers of unidirectional collagen fibrils (100 - 160 nm in diameter). Depending on the mineral distribution, the Elasmodine can be further divided into the External (EE) and Internal Elasmodine (IE). The EE is more highly mineralized due to an increased reinforcement of apatite platelets (Murcia et al. 2017). Collagen fibrils of the elasmodine are packed into larger fibers, which are aligned and assembled into individual unidirectional plies (or lamellae). The plies are stacked with a helicoidal arrangement commonly known as a Bouligand structure (M. A. Meyers et al. 2012).

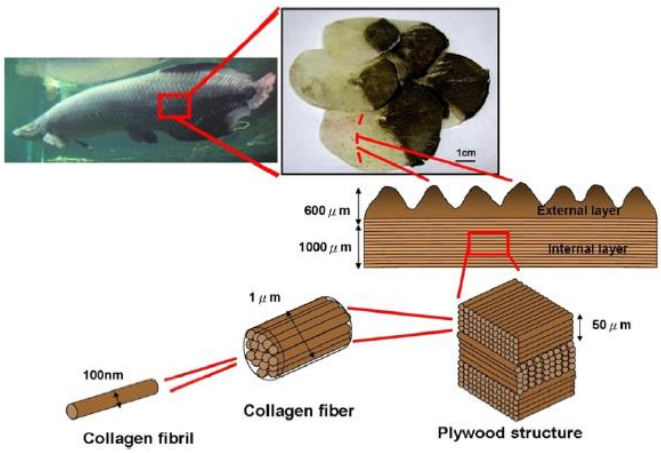

Figure 2.3 Hierarchical structure of the Arapaima gigas scale. Reproduced from: (Lin et al. 2011).

Interestingly, the Bouligand structure serves a critical role in the mechanical behavior of this material system by enhancing the ductility and toughness of scales (Zimmermann et al. 2013). Furthermore, the hierarchical structure facilitates the dissipation of energy across different length scale levels (Ghods et al. 2019; M. A. Meyers et al. 2012). At the macroscale (> 1 mm), the outer layer (LL) dissipates energy through mechanisms of brittle fracture, while the basal fibrous structure undergoes a high degree of deformation before failure (Arola et al. 2018). At the micro-scale (1 μm to 1 mm), the Bouligand arrangement facilitates a reorientation of the lamellae in response to the loading direction. Under in-plane tensile loads, deformation occurs through a combination of stretching and interfacial sliding mechanisms (Murcia et al. 2017; Zimmermann et al. 2013). And at the nano-scale (1 nm - 1μm), the collagen fibrils straighten, rotate, stretch, and eventually undergo fracture, a process that dissipates substantial energy. This process is accompanied by the resistance to sliding caused by the interfibrillar nanoscopic mineral platelets of apatite. As such, this behavior is highly dependent on the mineral content.

In mineralized tissues consisting of moderate mineral content, the collagen fibrils uncoil first and then increase their stiffness due to the stress transfer among the mineral platelets present (Huang et al. 2019). At the atomic scale (< 1 nm), the collagen molecules dissipate energy by uncoiling and through breaking and reforming of hydrogen bonds between molecular chains (Huang et al. 2019). This interplay between the different energy dissipation mechanisms allows efficient and light-weight protection against predation; however, these mechanisms are highly affected by the hydration level of the scales. Indeed, the stiffness, strength and toughness of the scales have shown to be highly dependent on water content (Lin et al. 2011; Murcia et al. 2016).

Like scales, osteoderms are natural protection systems configured in segmented arrangements; however, osteoderms are found in mammals and reptiles instead of fish. In contrast to scales, osteoderms are skin-covered bony plates connected by non-mineralized collagen fibers, arranged in juxtaposed arrays (Chen et al. 2011; Chen, Yang, and Meyers 2014, 2015; Damiens et al. 2012; C.-Y. Y. Sun and Chen 2013; Yang et al. 2012; Yang, Chen, et al. 2013; X. Zhang et al. 2018). These bony plates have a sandwich-like structure comprised of a dense outer sheath enclosing a porous core. Consequently, differences in porosity degree cause changes in the degree of mineral content (i.e., like scales, osteoderms also exhibit graded mineralization). Remarkably, this sandwich-like structure is also found in other biological and synthetic configurations in which low density, stiffness, and a moderate energy absorption capability is required (Yang, Chen, et al. 2013).

Alligators and Turtles are reptiles covered with osteoderms. As shown in Figure 2.4, Alligators have disk-like shape osteoderms linked together by flexible fibers connected through their smooth edges (Chen, Yang, and Meyers 2014; C.-Y. Y. Sun and Chen 2013).

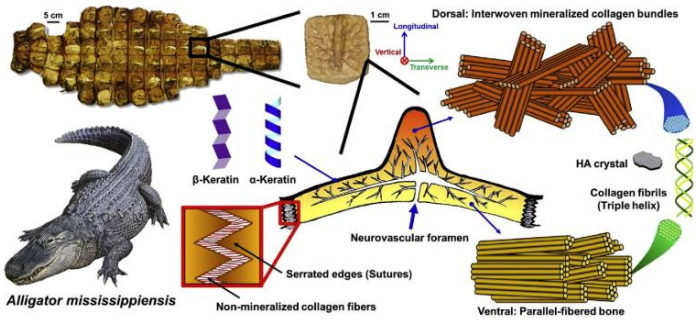

Figure 2.4 Hierarchical structure of the Alligator osteoderms. Reproduced from: (C.-Y. Y. Sun and Chen 2013).

On the contrary, As shown in Figure 2.5, Turtles carapaces are comprised of polygonal osteoderms separated by sutures providing restricted levels of flexibility (Chen, Yang, and Meyers 2015).

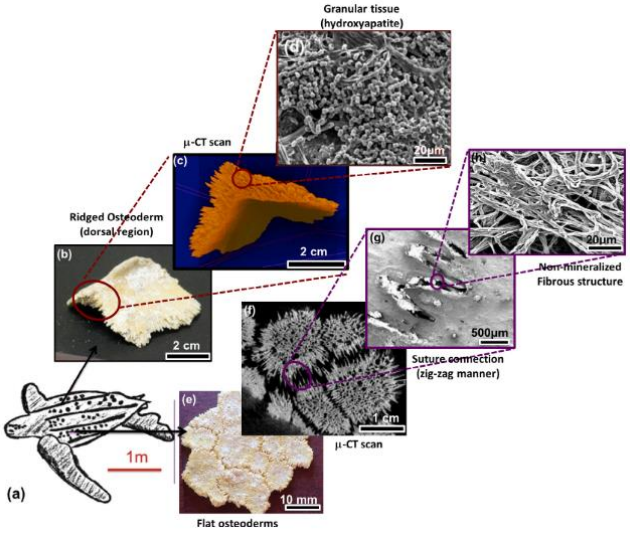

Figure 2.5 Hierarchical structure of the Leatherback Turtle osteoderms. Reproduced from: (Chen, Yang, and Meyers 2015).

Unlike these reptiles, armadillos are mammals covered in polygonal (i.e., hexagonal and triangular) osteoderms, but opposite to Turtles, the carapace of Armadillos is completely

separated from vertebrae and ribs, enabling flexibility (Chen et al. 2011). Armadillo osteoderms, are also organized in a hierarchical structure (Figure 2.6). The bony plates that protect armadillos are comprised mostly of a type I collagen fiber network and laterally oriented osteons, which are the fundamental basic unit of cortical bone. Osteons are configured as central vascular canals wrapped with concentrically oriented collagen fibers (lamellae).

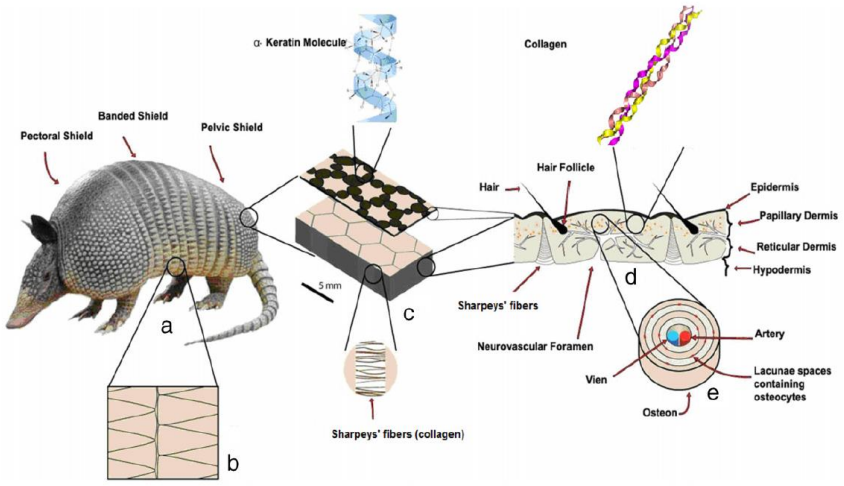

Figure 2.6 Hierarchical structure of Armadillo osteoderms. Reproduced from: (Chen et al. 2011).

Although limited hierarchical structures have been shown here (i.e., arapaima scales and armadillo osteoderms structures), this kind of arrangement is typical of all biological materials including the scales or osteoderms of Alligator Gars, Pangolins, Alligators, and Turtles (Allison et al. 2013; Chen, Yang, and Meyers 2014, 2015; Liu et al. 2016; C.-Y. Y. Sun and Chen 2013; Wang et al. 2016; Yang, Gludovatz, et al. 2013).

As shown above, segmented natural armor (i.e., protective systems based on scales and osteoderms) present major differences between different animals, therefore, Table 2.1 summarize the main geometrical, compositional and mechanical aspects comprising the

protective systems of Arapaimas, Alligator Gars, Pangolins, Alligators, Leatherback Turtles, and Armadillos.

Table 2.1 Summary of the geometrical, compositional and mechanical properties of selected natural armor. Modulus corresponds to the approximate values of Young modulus. Young modulus for Alligator gar corresponds to the ganoine layer.

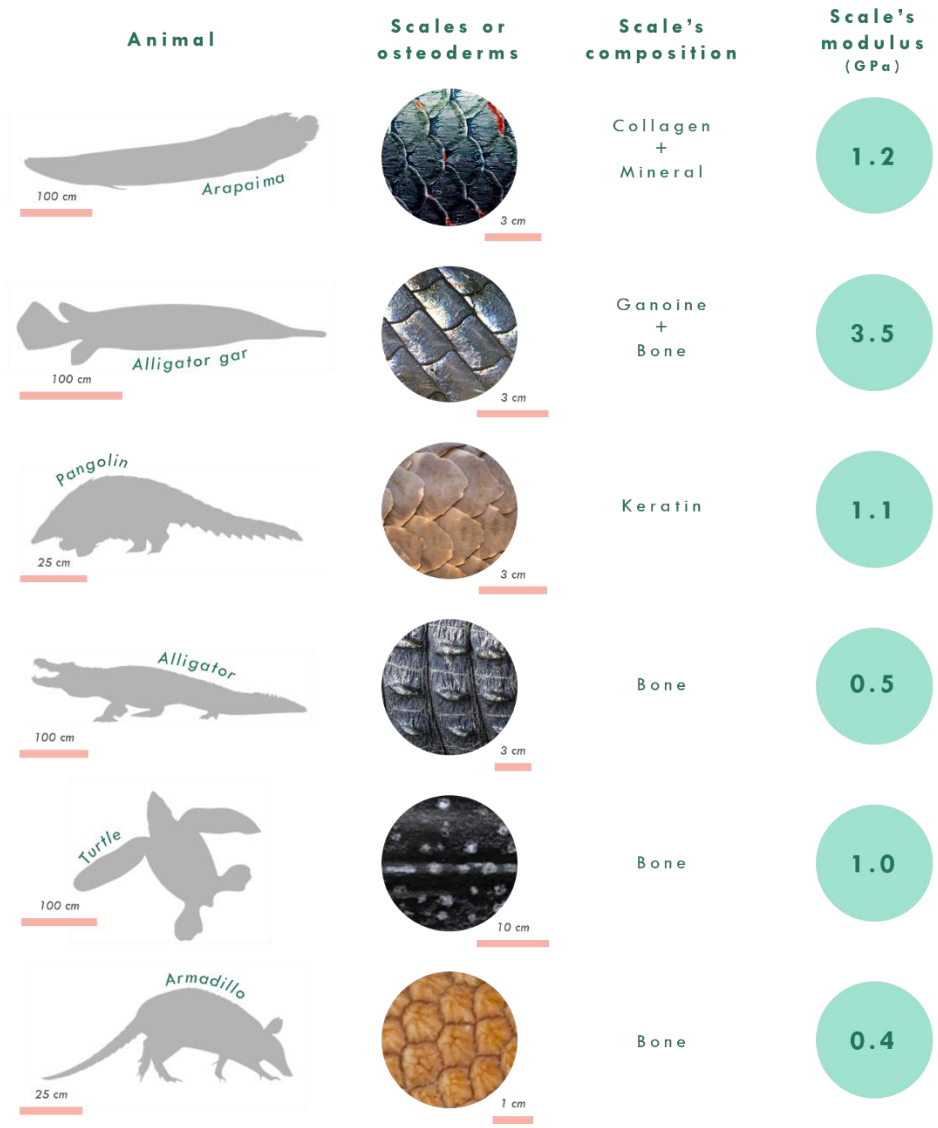

Despite the clear differences between scales and osteoderms described in Table 2.1, it is noteworthy that they share some structural commonalities: they are arranged in

segmented configurations, exhibit hierarchical structures, and most of them present graded mineralization. By using biomimetics, some of these aspects have been used to develop synthetic protective systems as shown in the following Section.

2.2 Biomimetics for protective applications

Since mythical and ancient times nature has inspired the solution of technical problems (Volstad and Boks 2012). This discipline is known as biomimetics and has been applied in a wide range of applications (Shu et al. 2011). In architecture, biomimetics has guided the development of buildings with regulated temperature decreasing the investment in air conditioning systems (Radwan and Osama 2016; Zuazua-Ros et al. 2017). Nature has also guided textiles design, where the structure of scales found in sharks and rays have inspired the development of fabrics that can reduce drag in water (Han et al. 2016). Even in medicine biomimetic design methodologies have been used to develop bioinspired drug delivery systems mimicking features found in natural components of the body (Sabu et al. 2018).

One of the main obstacles when using biomimetic methods is related to the transference of biological knowledge into technical concepts, due to the difference of terminology used by engineers and biologists (Fayemi et al. 2017; Shu et al. 2011). To close this gap many biomimetic strategies have been proposed including graphic tools such as BioCards, and TRIZ-based methods where the design process is guided by a previous study of contradictions and solutions found in biological systems (T. Lenau et al. 2010; Vincent et al. 2006). Besides methodological differences, most approaches agree on the importance of describing the functional principles that govern the natural phenomena that are being

mimicked. Further discussion about biomimetics, its methods and tools is described in Chapter 3.

Most of the efforts to develop bioinspired protective systems have been focused on mimicking the brick and mortar arrangements found in nacre (Askarinejad and Rahbar 2018; Gu, Takaffoli, and Buehler 2017; Mirkhalaf, Tanguay, and Barthelat 2016), cross-ply laminar composites and overlapping configurations like those found in fish scales (Grunenfelder et al. 2014; Martini and Barthelat 2016a; Rudykh, Ortiz, and Boyce 2015; Zhen Yin, Dastjerdi, and Barthelat 2018), and assembled tubular sections following the structure of tendons and muscles (Tsang and Raza 2018).

A recurring characteristic among these bioinspired protective systems is the introduction of hierarchy at micro and macro scales (Marc André Meyers et al. 2008). However, while man-made materials can only reach up to three orders of hierarchy, biological materials exhibit between four and eight levels of hierarchy (Marc A. Meyers et al. 2011). This limitation is often associated with length scale restrictions of the manufacturing processes that are frequently narrowed to the micro and the macro scales (i.e., 3D printing and laser engraving). Nevertheless, recent studies have improved the toughness and strength of synthetic materials, by mimicking nacre and natural interfaces at the nanoscale (Burghard et al. 2009; Li et al. 2015; Song et al. 2018; Y. Zhang and Li 2017).

Another recurring characteristic among the bioinspired protective systems is segmentation. As described in Section 2.1, segmentation is one of the main principles found in segmented natural armor. In these natural configurations, rigid units distribute puncture loads over broader areas reducing stress concentration, whereas the interconnecting flexible fibers allow flexibility (Yang, Chen, et al. 2013). Usually, this

segmentation occurs at length scales that range between the microscale and the size of the animal (i.e., the mesoscale), comprising one of the main attributes of architectured materials. These distinctive arrangements are common in biology and engineering and are characterized by presenting atypical behaviors when compared with non-architectured structures (F. Barthelat 2015; Reis, Jaeger, and van Hecke 2015). For instance, the introduction of mesoscopic repetitive patterns in elastic membranes can generate auxetic behaviors (i.e. materials with a positive Poisson's ratio) (Eidini 2016; Rafsanjani and Pasini 2016; Shan et al. 2015). Figure 2.7 shows some of the repetitive patterns used in these studies, often inspired by ancient architecture.

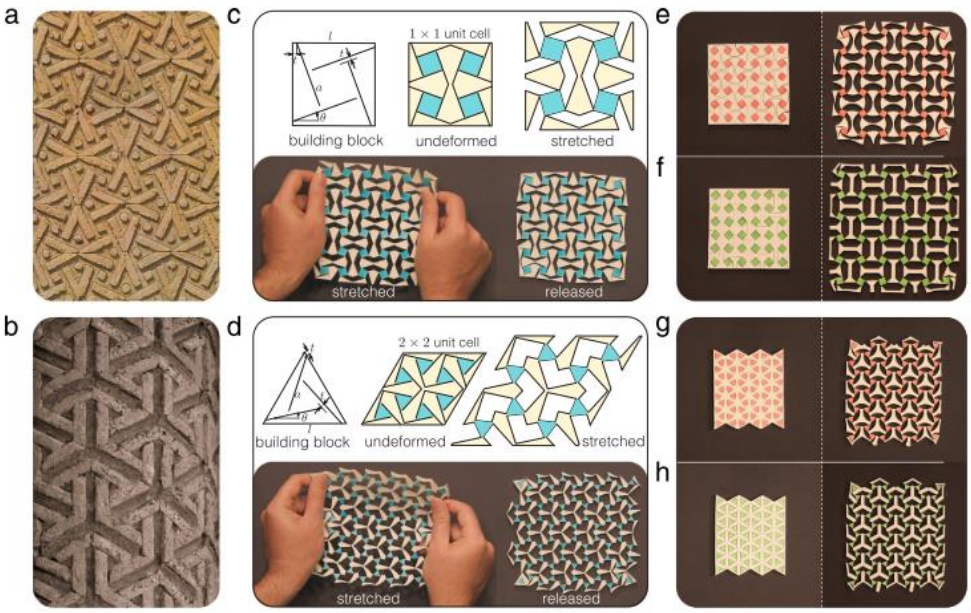

Figure 2.7 Bistable auxetic materials. Reproduced from: (Rafsanjani and Pasini 2016).

The mechanical performance of architectured materials relies on the control of geometrical parameters since they govern the mechanisms of deformation and failure of the material. To control geometry across manufacture, two different fabrication strategies

have been used: Bottom-up and Top-down fabrication approaches. The Bottom-up fabrication approach consists of assembling disordered elements into ordered structures, while in Top-down approaches the architectures are carved in the bulk of monolithic materials (F. Barthelat 2015).

In the next section some examples of bioinspired protection systems are described and classified according to their fabrication approach.

2.2.1 Segmented armor development using bottom-up fabrication approaches

To duplicate the toughening mechanisms found in nacre, Barthelat and Zhu manufactured a prototype consisting of wavy polymeric tablets held by fasteners (See Figure 2.8). This material experimented a high tablet sliding under tensile loads, accompanied by strain hardening similar to natural nacre (F Barthelat and Zhu 2011).

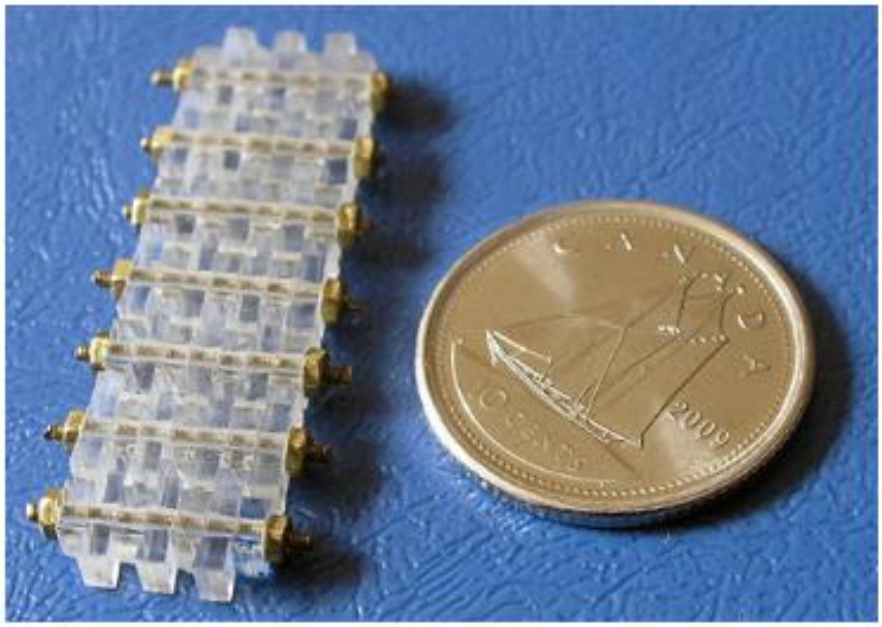

Figure 2.8 Wavy polymeric tablets held by fasteners mimicking the structure found in Nacre. Reproduced from:(F Barthelat and Zhu 2011).

For high demanding impact applications such as ballistic threats, researchers developed a Nacre-like composite comprised of aluminum alloy platelets bonded together with an epoxy adhesive (see Figure 2.9) (Miao et al. 2019).

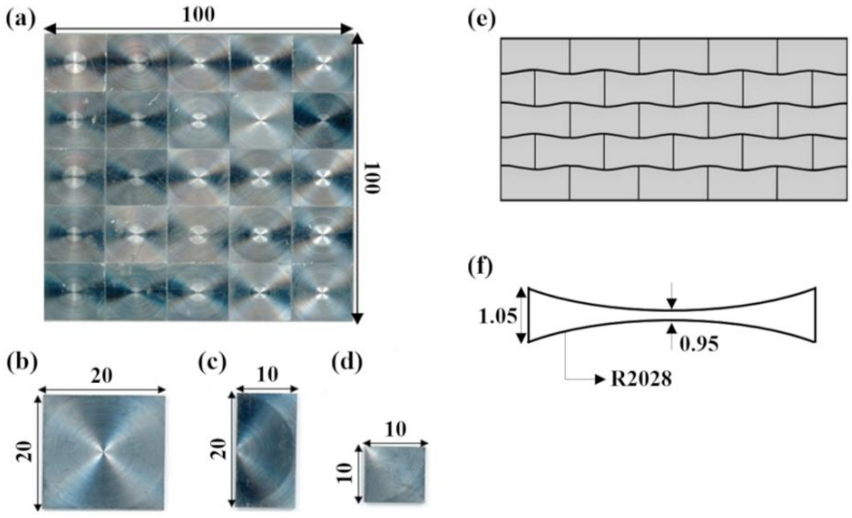

Figure 2.9 Nacre-like aluminum composite for ballistic applications. Reproduced from: (Miao et al. 2019).

Likewise, 3D printing has been used to mimic scaled skins (Browning, Ortiz, and Boyce 2013). As shown in Figure 2.10 a group of researchers tested under puncture a 3D printed stiff plate – soft matrix material revealing the ability of these systems to protect while preserving flexibility (Rudykh, Ortiz, and Boyce 2015).

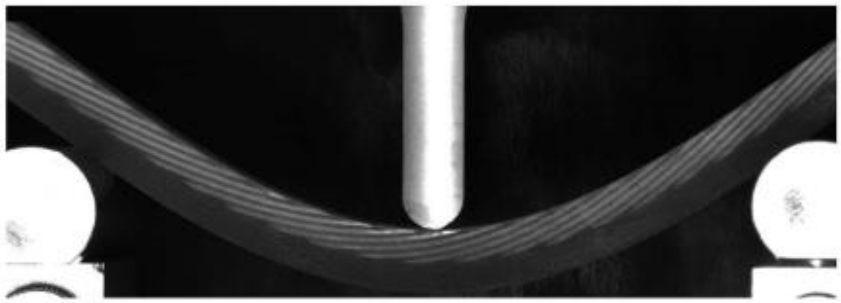

Figure 2.10 3D printed hybrid material under puncture load. Reproduced from:(Rudykh, Ortiz, and Boyce 2015).

Similarly, Martini et al. presented 3D printed arrays of scales (Figure 2.11), varying from simple arrangements with no overlaps to complex and interlocked configurations inspired by ganoid and teleost scales (Martini, Balit, and Barthelat 2017). Results from puncture tests suggested that natural evolution shaped scaled systems to maximize flexible protection.

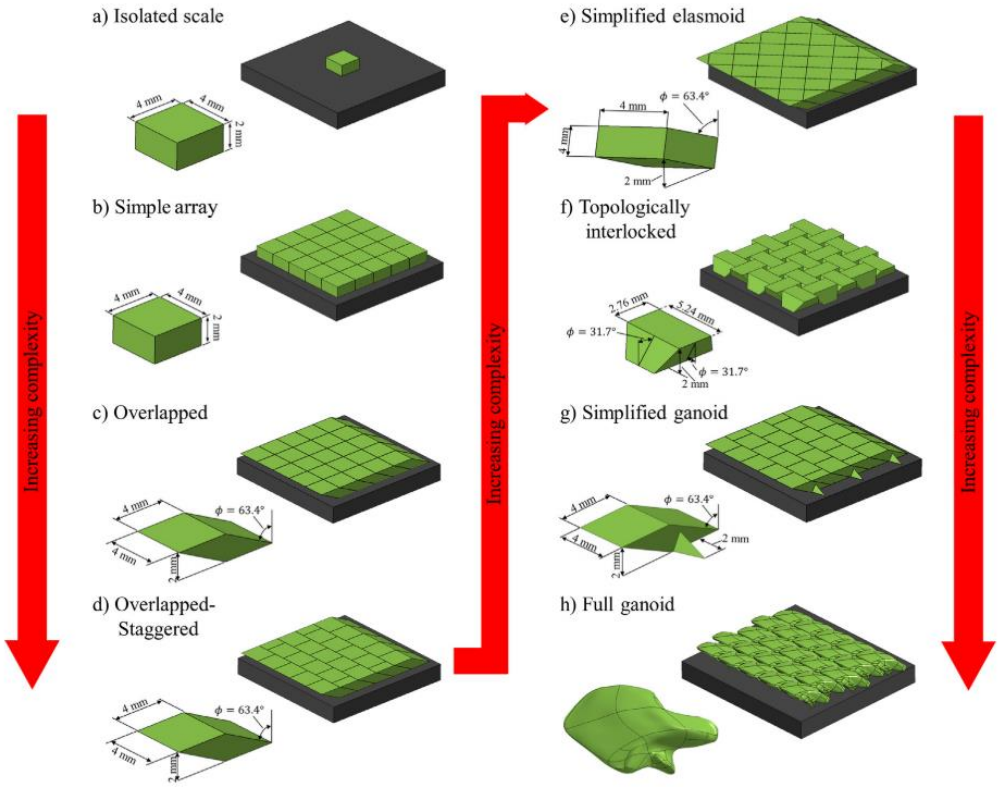

Figure 2.11 3D printed scale systems with different levels of complexity. Reproduced from: (Martini, Balit, and Barthelat 2017).

Besides using 3D printing to replicate segmented arrangements, it has also been used to introduce new levels of hierarchy in synthetic materials. Gu, Takaffoli and Buehler proposed a hierarchically enhanced 3D printed composite showed in Figure 2.12 that

improved its impact resistant capabilities up to 70% and 85% when new levels of hierarchy were introduced.

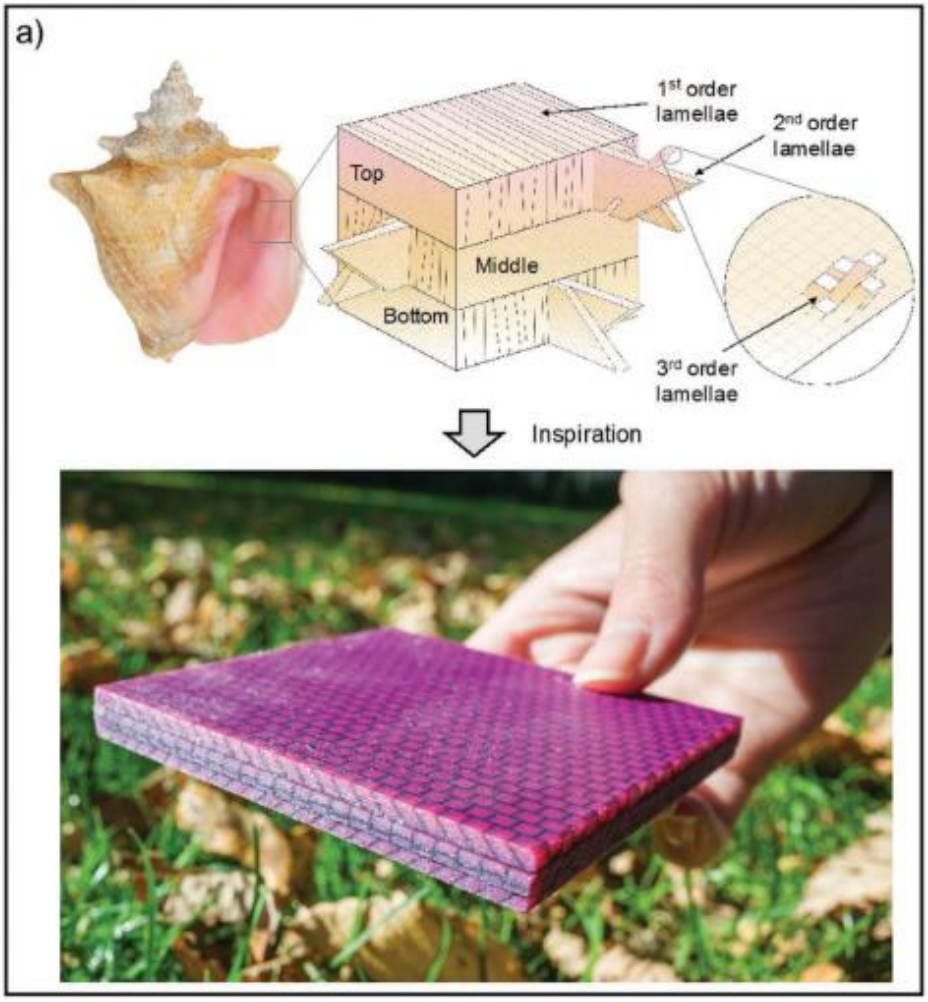

Figure 2.12 3D printed Conch shell inspired structure. Reproduced from: (Gu, Takaffoli, and Buehler 2017).

As shown, 3D printing has been widely used to emulate nature's complex arrangements due to their high geometrical control, however, its application in industrial scenarios is limited due to their associated added costs. Besides, 3D printing has limitations to introduce hierarchy at submillimeter scales.

2.2.2 Segmented armor development using top-down fabrication approaches

Laser engraving has been widely used for introducing architectures into bulk materials. Nacre-like materials have been widely developed using this technic generating interconnected wavy platelets and topologically interlocked structures in glass-based materials (Valashani and Barthelat 2015). Likewise, the impact resistance of glass was enhanced by including segmented and hierarchical arrangements when combining laser engraving with polymeric substrates (see Figure 2.13) (Mirkhalaf, Tanguay, and Barthelat 2016; Z Yin, Hannard, and Barthelat 2019).

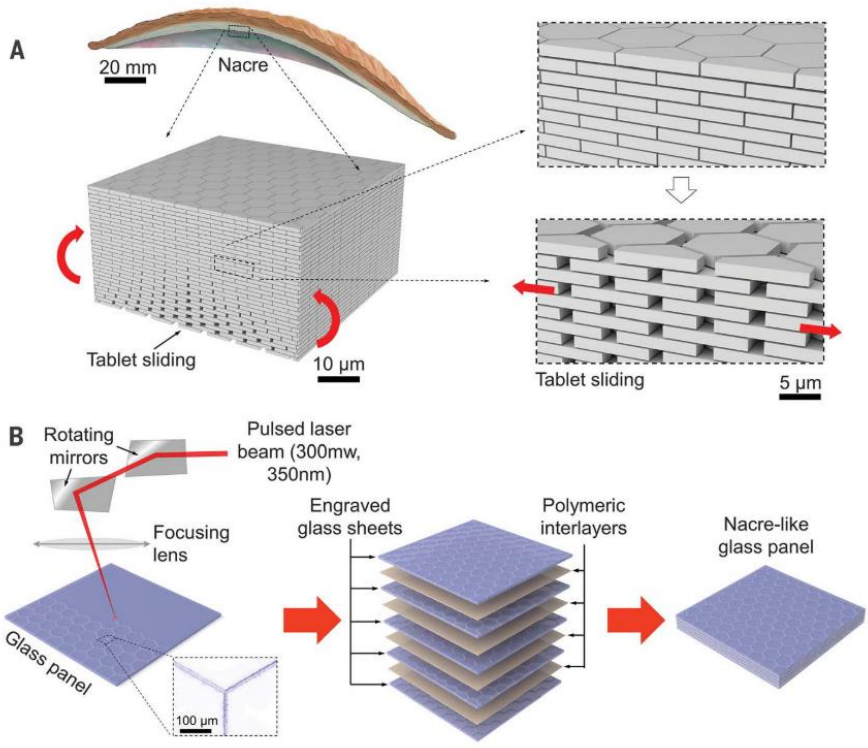

Figure 2.13 Laser engraved Nacre inspired structure. Reproduced from: (Z Yin, Hannard, and Barthelat 2019).

Finally, by carving hexagonal units in plain glass, researchers mimicked the juxtaposed arrangements found in osteoderms improving the puncture resistance of bioinspired arrangements when smaller hexagons were used (see Figure 2.14) (Chintapalli et al. 2014).

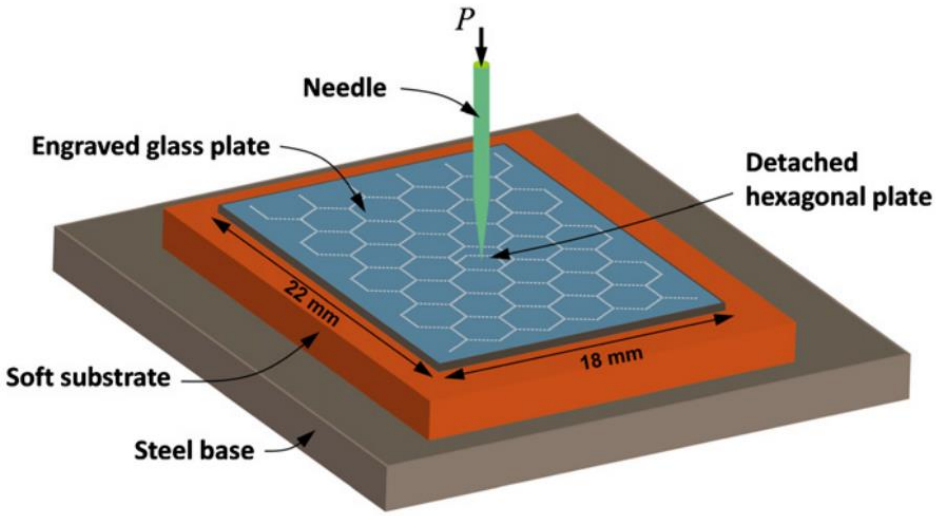

Figure 2.14 Glass engraved with hexagonal arrangements under puncture loads. Reproduced from: (Z Yin, Hannard, and Barthelat 2019).

As shown, laser engraving has been widely used to introduce bioinspired arrangements in glass-based materials providing a low-cost route to include high-precision bioinspired patterns in bulk materials.

2.2.3 Segmented armor development using other fabrication approaches

By using a combination of top-down and bottom-up fabrication approaches, a novel fabrication approach was recently proposed Martini and Barthelat (see Figure 2.15). This technic was termed as stretch-and-release and enables the reproduction of tunable overlapped ceramic arrangements (Martini and Barthelat 2016b).

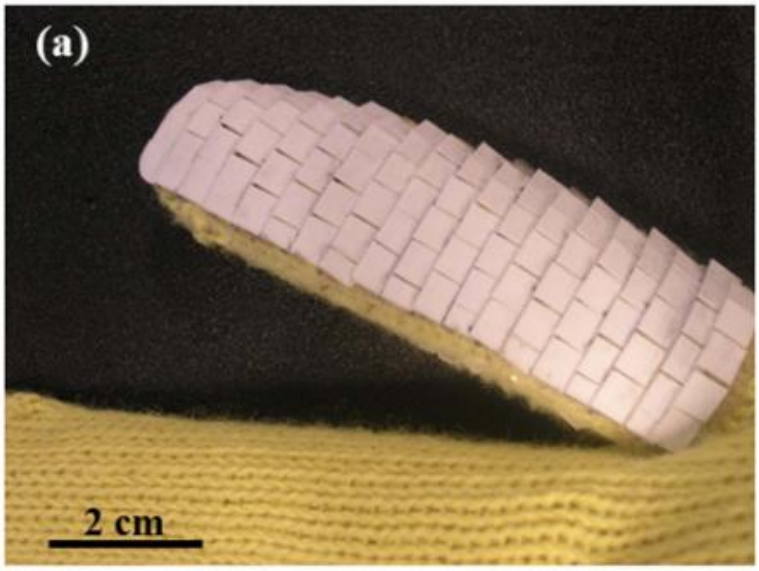

Figure 2.15 A Kevlar glove partially covered with a synthetic scaled system fabricated using stretch-and-release. Reproduced from: (Z Yin, Hannard, and Barthelat 2019).

Although simulation is not a fabrication technique, it can be used to understand mechanisms and functional principles governing segmented natural armor. For instance, through the use of simulation, Jayasankar et al. (2017) proposed a model to understand the mechanical behavior of bioinspired composites. Other simulation-based works focused on developing computational models to adapt segmented armor (Duro-Royo et al. 2015), and likewise, a recent study focused on unraveling the influence of waviness and geometry in idealized suture systems (Gao and Li 2019).

2.3 Concluding remarks

Segmented natural armor is an extraordinary protective system found in different animal species including mammals, reptiles and fish. These arrangements are characterized by protecting against high predatory threats while enabling flexibility necessary for

locomotion. Despite their differences, these arrangements share common functional principles like segmentation, structural hierarchization and graded mineralization. By using biomimetics, some of these principles have inspired researchers in the last decades to develop extraordinary synthetic arrangements (e.g., laser engraved nacre-like arrangements, 3D printed scaled systems). However, while these studies help to establish the promise of bioinspired concepts in materials development, most of these concepts are far from industrial scalability due to their high added costs. Moreover, most of these approaches do not provide clear guidance to transfer the biological principles into synthetic industrially scalable configurations. Therefore, new methods and tools are necessary to provide clear guidance in bioinspired design processes.

Chapter 3: A simplified recipe for bioinspired design

As briefly discussed in the second Chapter, biomimetics is a discipline that seeks to transfer the design lessons of nature into synthetic configurations. However, this is a challenging task for both engineers, biologists and designers. This Chapter provides an overview of some tools and methods used in this field of study. Moreover, it presents some of the common misunderstandings between biomimetics and its closest relatives: bionics and biomechanics. Then, by showing some successful biomimetic developments, this Chapter proposes that simplification can be the cornerstone for biomimetics popularization. Finally, a simplified methodology for biomimetic design is proposed and used to conceptualize design ideas for flexible protection.

3.1 Lost in translation

Since the most primitive origins (i.e., 3.8 billion years ago) living beings have faced countless design challenges to survive environmental threats and thus, nature provides multiple examples of highly efficient systems that resemble solutions to technical problems. This is in fact, one of the main assumptions of biomimetics: nature is a master of design (Bar-Cohen 2006; Francois Barthelat 2007; Bhushan 2009; M. Helms, Vattam, and Goel 2009; Shu et al. 2011).

By definition, biomimetics moves between two different domains of knowledge (i.e., engineering and biology) generating an ideal environment for the emergence of new ideas.

Consequently, biomimetics has grown significantly as a field of study in the last decades, providing novel solutions in different areas such as architecture, medicine and textiles design. However, its inter-disciplinary nature can generate implementation difficulties in industrial scenarios (M. Helms, Vattam, and Goel 2009; Lepora, Verschure, and Prescott 2013; López et al. 2017; Sabu et al. 2018). As a consequence, many tools and methodologies for bioinspired design have been recently developed aiming to reduce the gap between biologists and engineers (Glier, McAdams, and Linsey 2011; M. Helms and Goel 2014; T. Lenau et al. 2010; T. A. Lenau et al. 2015; Torben Lenau 2009; Volstad and Boks 2012; Wanieck et al. 2016).

In general, bioinspired design methodologies follow two types of approaches, the first one focuses on the biological solution (i.e., solution-based approach), while the second concentrates its efforts on the design problem (i.e., problem-driven approach). The main difference between them being their starting points. While a solution-based approach is initiated by the knowledge of a biological phenomenon, a problem-driven approach is started by identifying a technical problem. Therefore, in the first approach a deep understanding of the biological phenomena is needed since technology is meant to emulate it. On the contrary, the second approach focuses on defined technological challenges, and as a consequence, the examined biological phenomena are chosen according to their resemblance to the expected technical performance. Both types of approaches have generated remarkable biomimetic developments. Velcro® is an example of a widely known biomimetic development designed through a solution-based approach. In 1948, Swiss engineer George de Mestal noticed that some seeds enable an instant grip on clothes. This idea led to the invention of a zip called Velcro®, which works as a zipper (Bhushan 2009).

Despite the usefulness of a solution-based approach to developing successful designs, the problem-driven approach is closer to industrial developments, since industrial challenges usually present technical problems as starting points (Fayemi et al. 2017; M. Helms, Vattam, and Goel 2009). Therefore, the simplified bioinspired methodology proposed here uses a problem-driven approach.

Recent studies have proposed different problem-driven methodologies to assist the nature-inspired design (Cheong et al. 2011; M. E. Helms et al. 2008; T. Lenau et al. 2010; Lindemann and Gramann 2004; Nagel et al. 2010). Recently, a group of researchers summarized many of the current methodologies in a single study identifying general problem-driven processes (i.e., identification, definition, alternative generation, choice of a solution, implementation and testing, and further steps) as shown in Figure 3.1 (Fayemi et al. 2017).

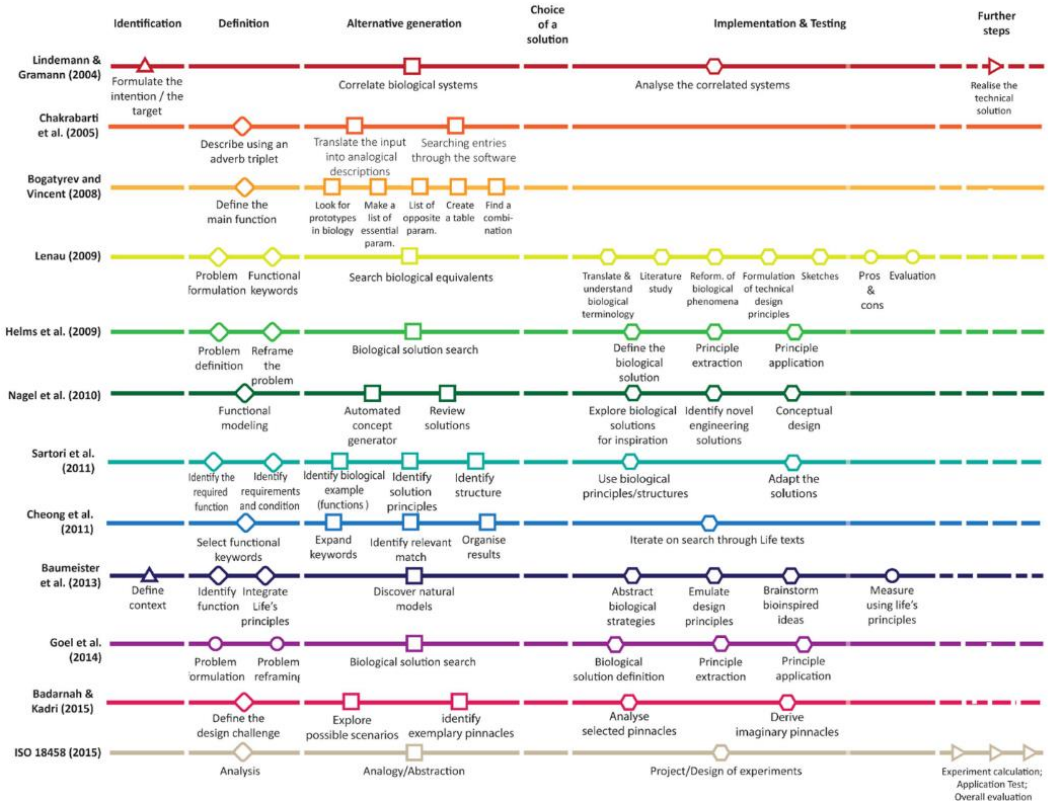

Figure 3.1 Problem-driven biomimetic process models correlated with general problem-driven processes. Reproduced from: (Fayemi et al. 2017).

Besides, Fayemi et al. proposed a unified methodology consisting of the following eight steps:

1) Problem analysis.
2) Abstract the problem.
3) Transpose to biology.
4) Identify potential models.
5) Select models of interest.
6) Abstract biological strategies.
7) Transpose to technology.
8) Implement the initial context.

Instead of being linear, the unified methodology proposed by this study is abstracted as a double symmetrical cycle as shown in Figure 3.2.

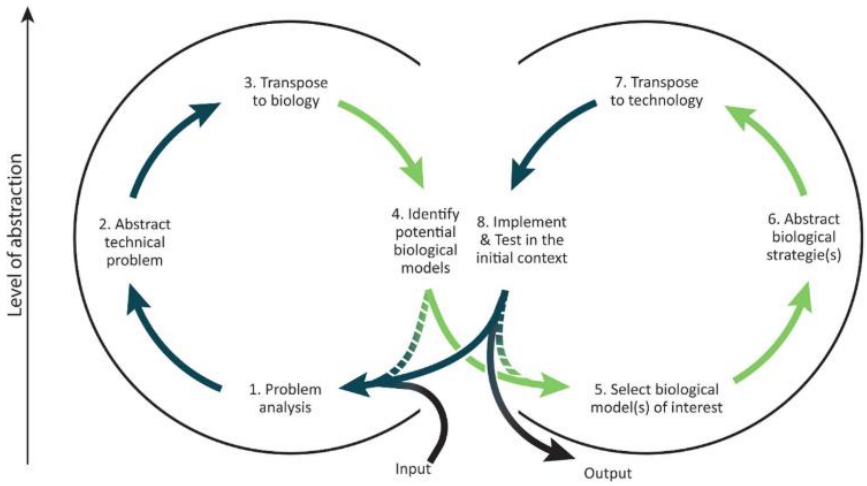

Figure 3.2 The unified problem-driven process of biomimetics. Reproduced from: (Fayemi et al. 2017).

Finally, a biomimetic utility tree was also provided showing the current tools available for each step of the unified biomimetic methodology (see Figure 3.3).

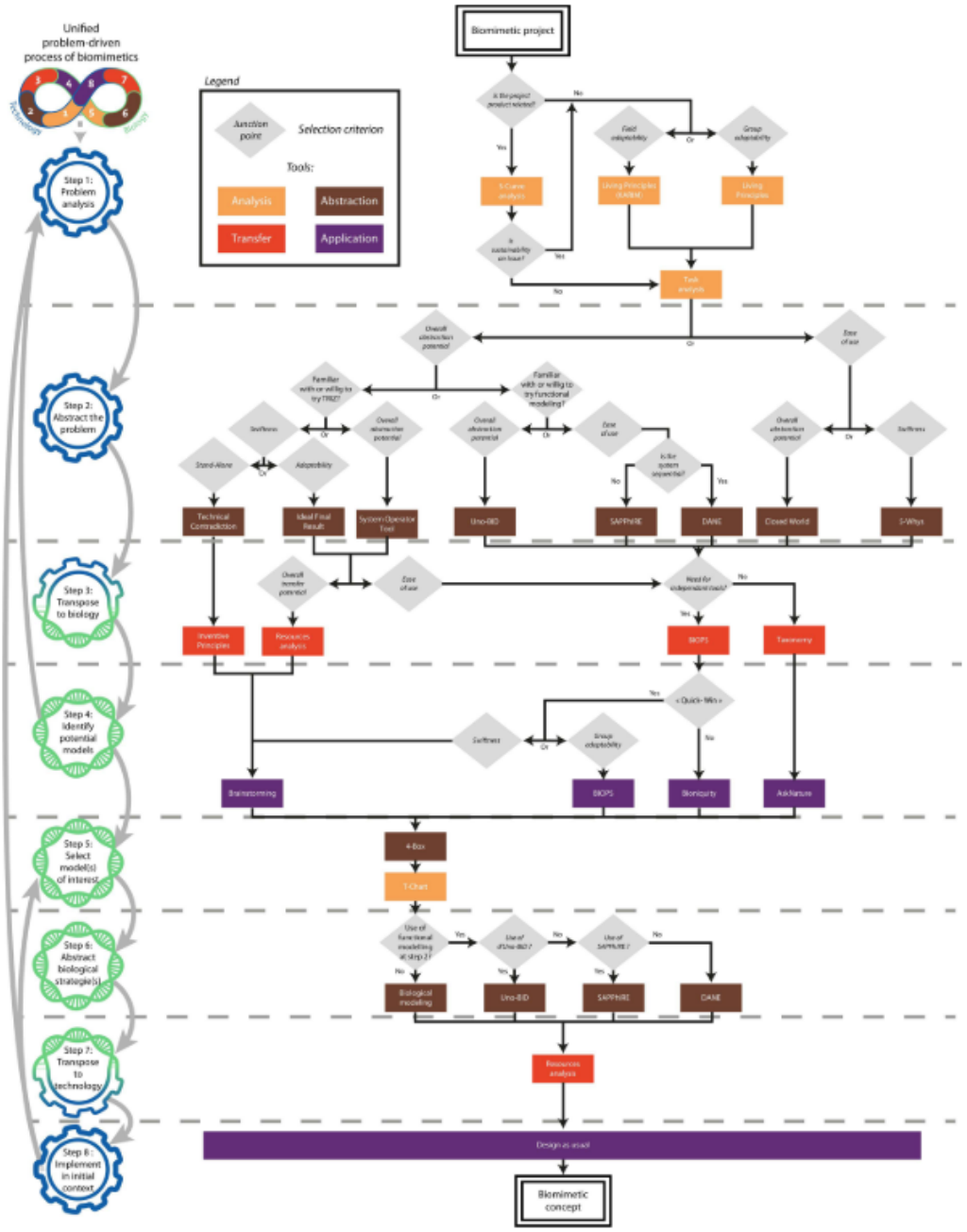

Figure 3.3 Utility tree of biomimetic tools associated with biomimetic process steps. Reproduced from: (Fayemi et al. 2017).

Researchers identified up to 23 different biomimetic tools separated into four conceptual categories: *i*) analysis tools, *ii*) abstraction tools, *iii*) transfer tools, and *iv*) application tools. Analysis tools are meant to define the problem space, abstraction tools focus on generating analogies between technology and biology, transfer tools are meant to transpose concepts from biology to technology, and finally, application tools seek concretization.

Despite these efforts of unifying the existing biomimetic toolbox in a unique methodology, the use of bioinspiration in real design challenges is still limited. This dissertation proposes that this limitation is caused by two different sources: Firstly, there is a conceptual misunderstanding around biomimetics (and its relatives), and secondly, the extensive number and complexity of biomimetic tools can be overwhelming for non-specialized audiences.

3.2 Common misunderstandings around biomimetics

As stated before, there is a common misunderstanding between biomimetics and its closest relatives: bionics and biomechanics. Contrary to Biomimetics, Bionics is a discipline that aims to replicate the exact design of nature (e.g., robots that swim like fish). These works represent a huge mechatronics challenge; nonetheless, they are not Biomimetics!. Biomechanics on the other hand, focus on analyzing the mechanical phenomena behind a biological fact (e.g., how scales surface may affect the swimming efficiency of a certain fish species). Biomechanics usually represents a great source of information for biomimetics; however, they configure different disciplines. Instead, biomimetics seeks to solve technical or industrially relevant problems by using design concepts extracted from

biology. Moreover, instead of copying biology, biomimetics has the license to abstract or idealize biological functional principles to enable its transference to technology. Successful biomimetic developments may elucidate this idea.

3.3 Simplification, the cornerstone of biomimetic design

As mentioned before, Velcro ® is a well-known biomimetic development inspired by the complex superficial structures found in some seeds. The mentioned seed is covered with microscopic hairs that anchor to other hairy structures (e.g., the hairy skin of mammals) to be dispersed. However, this biological complexity is not exactly replicated by Velcro®, instead, Velcro® uses a simple idea: microscopic hook-like surfaces get easily attached to woolly substrates. This simplification and not the actual biological phenomena (i.e., complex surfaces in seeds to enable propagation), is emulated by Velcro® (see Figure 3.4).

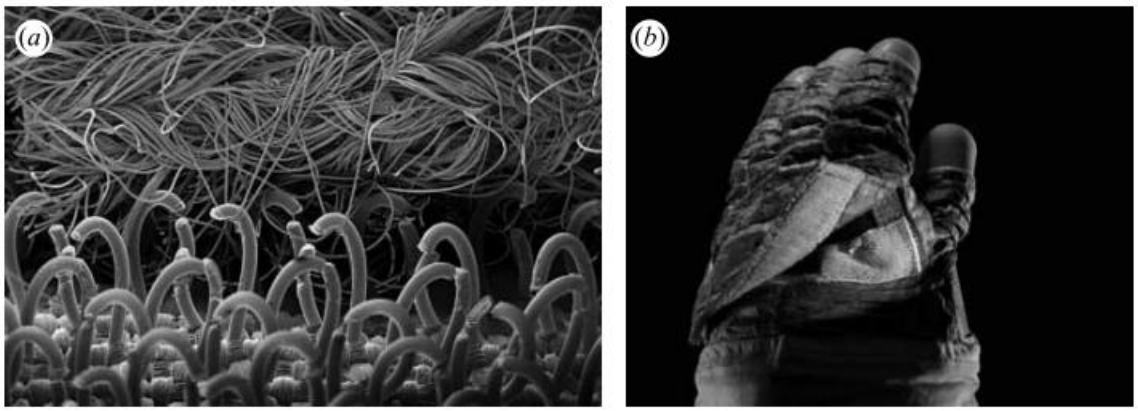

Figure 3.4 (a) Micrographs of the tiny hooks found in cockleburs and (b) commercial Velcro®. Reproduced from: (Bhushan 2009).

Another common example of a successful biomimetic development is a swimsuit developed by Speedo called Fastskin bodysuit. Drag in water is a major hindrance to the movement for both swimmers and fish. Therefore, by knowing that shark scales could reduce drag in water from 5 to 10 %, Speedo designers developed Fastskin (Bhushan 2009). Sharks are covered with very small tooth-like scales called dermal denticles. These individual scales are ribbed with longitudinal grooves (i.e., aligned parallel to the local flow direction of the water), which results in efficient water moving over their surface. An example of this scaled structure is shown in Figure 3.5.

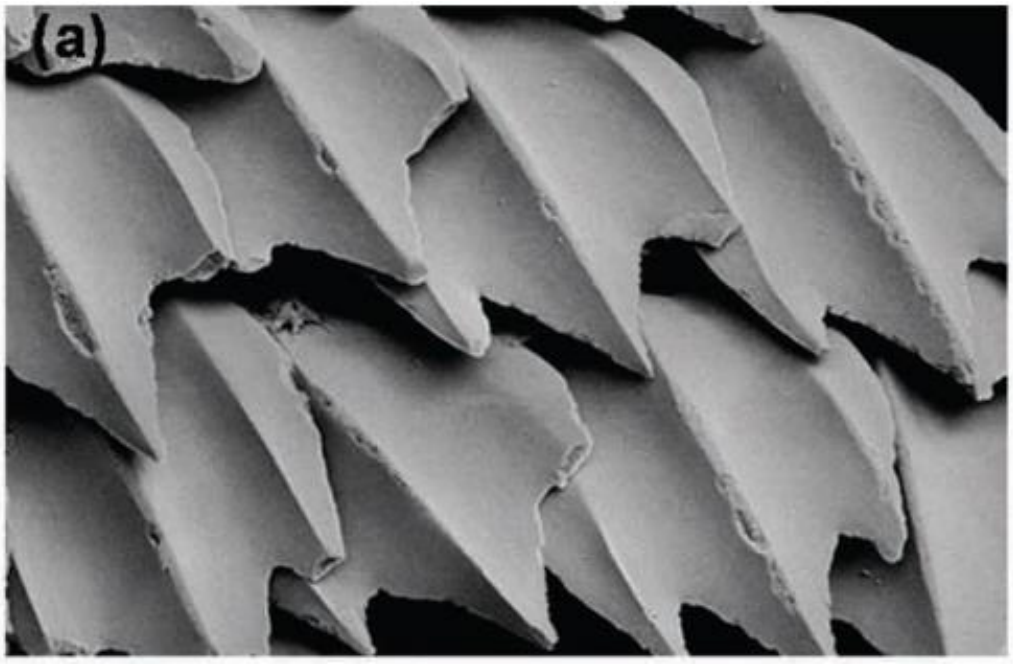

Figure 3.5 Placoid scales. Reproduced from: (Yang, Chen, et al. 2013).

Again, instead of mimicking the complex overlapping structure of shark scales, Fastskin emulates a simplified concept: small longitudinal grooves oriented parallel to the water flow can reduce drag.

Likewise, a simplified biological principle aid to increase the efficiency of energy production of wind turbine blades. Humpback whales have scalloped edges with a unique series of bumps called tubercles on their flippers which enable very tight turns (Bhushan 2009). Inspired by this, turbine blades with tubercles were designed (see figure 3.6), obtaining a reduction of wind drag and an increment of the angle of attack, thus increasing the efficiency of the wind turbine blades.

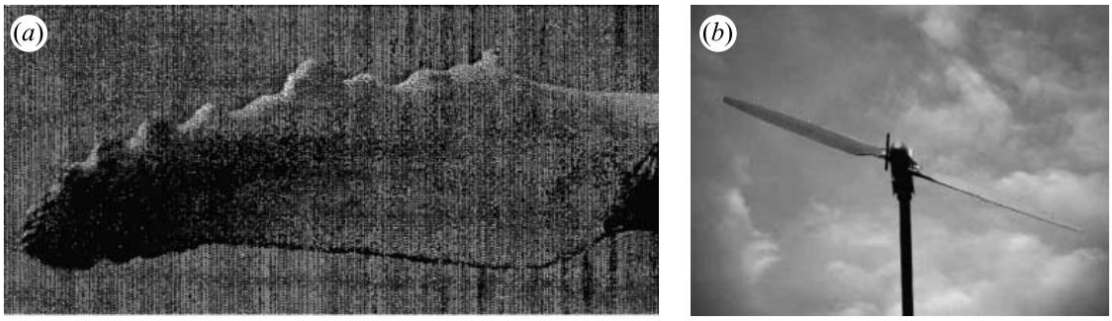

Figure 3.6 (a) Scalloped of humpback whale flippers, (b) turbine blades with tubercles to reduce drag in wind. Reproduced from: (Bhushan 2009).

Once again, instead of mimicking the exact design of nature with irregular tubercles, a simplified concept was emulated by this biomimetic wind blade: scalloped edges can reduce drag in wind.

Based on the analysis of these successful biomimetic developments and encouraged by the idea that design is mostly moved by curiosity and wonder (instead of being moved by overwhelming methodologies), this work proposes that simplification can be key to popularize the use of biomimetics.

3.4 A simplified methodology for bioinspired design.

While this section presents a simplified methodology for bioinspired design, the next section focusses on using it to develop bioinspired flexible protection. Although used specifically for flexible protection design, it is envisioned that this methodology can be useful in solving all kinds of technical problems, bringing the design lessons of nature into everyday devices.

As sown in Figure 3.7 the simplified methodology proposed here consists of four steps:

1) Define.

2) Search.

3) Simplify.

4) Conceptualize.

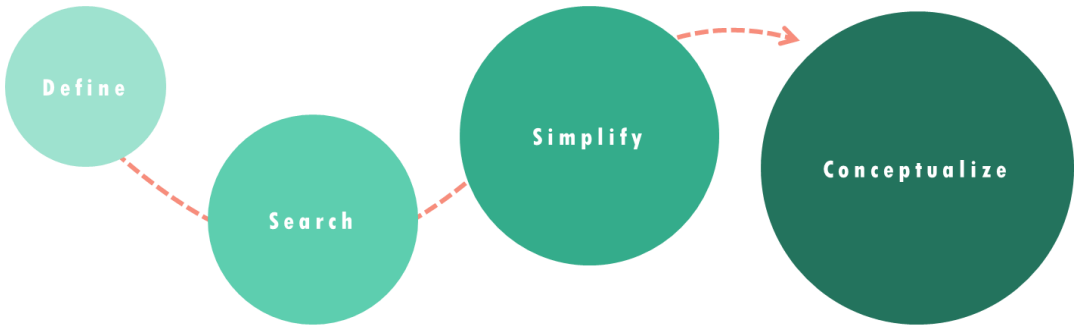

Figure 3.7 Simplified biomimetic methodology divided into four steps: define, search, simplify, and conceptualize.

3.4.1 Define

To solve a problem (of any kind), it is usual to start from establishing which is its nature and scope, therefore, this phase of the methodology seeks to clarify and narrow the design challenge. For product design there are multiple technics to establish a problem definition,

however, as this methodology seeks to be friendly for non-specialized audiences, an intuitive tool known as the four-box method is recommended (M. Helms and Goel 2014). Here, the technical problem is described in the following four categories:

1) *Function*: It consists of describing the actions (verbs) that the designed system must achieve.
2) *Operational Environment*: It refers to the locations, conditions or entities that interact with the designed system during its operation.
3) *Restrictions/Specifications*: Generally, these restrictions or specifications are related to the manufacturing process or the designed device itself. They include expected attributes such as material properties, shape, dimensions, physical characteristics, components and relationships between components.
4) *Performance criteria*: It consists of explaining the degree to which the new design is anticipated to perform its function and how to be judged as a good solution.

This tool seeks to summarize the limits and objectives of the design challenge, obtaining a good starting point to solve it.

3.4.2 Search

The phase "search" seeks to provide relevant biological models to be mimicked by technology. Here, the search would focus on finding biological organisms, processes, mechanisms, or ecosystems that resemble the function that was defined in the previous phase. A common tool to use here is Asknature.com, which is the largest database related to bioinspiration. It provides information about biological phenomenon and links to potential design ideas and applications (Fayemi et al. 2017). Besides using Asknature.com,

a further search in scientific databases is also recommended. To perform a valuable search, relevant keywords are essential. Although keywords are specific to each type of problem, words that summarize the expected function are a good starting point. According to the problem definition, the resulting biological models can be filtered aiming to select the most relevant.

3.4.3 Simplify

Simplification comprises the main goal of this methodology. Here, the biological models are analyzed aiming to abstract the functional principles that underlay their performance. Here, a functional principle is defined as the basic concept that allows a biological phenomenon to perform in a certain way. The use of images or drawings that represent functional principles can be useful in this stage. Presumably, this is the reason why many studies related to bioinspired design encourage the use of BioCards since they graphically summarize functional principles underlaying biological phenomena (T. Lenau et al. 2010; T. A. Lenau et al. 2015; Volstad and Boks 2012).

3.4.4 Conceptualize

Instead of providing an identical copy of the identified functional principles, biomimetics have the license to adapt them easing its transference to manufacturability. Here, the design task consists of generating design ideas that mimic the functional principles by using current manufacturing processes. However, this does not exclude the emergence of novel manufacturing technics during the biomimetic process. The resulting design ideas are the starting point for fabrication and testing; however, these exercises are

no longer the domain of biomimetics. Therefore, the simplified methodology for bioinspired design meets here its final phase.

3.5 Bioinspiration for flexible protection

Following the simplified methodology for bioinspired design presented above, this section illustrates how it can be used to develop flexible protection systems.

3.5.1 Define

By using the four-box method described above, a brief definition of the problem was obtained (see Figure 3.8). This friendly tool provides a brief framework to limit the scope of the design problem.

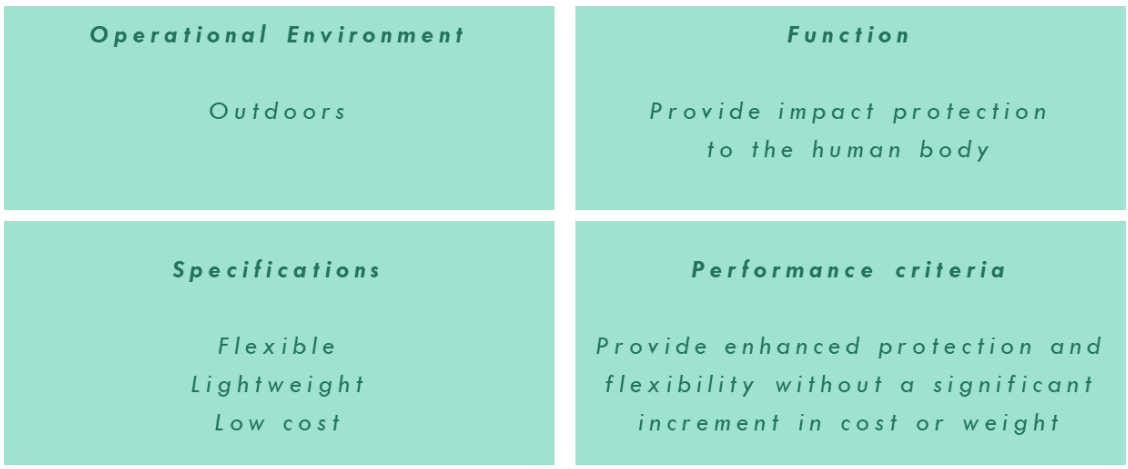

Figure 3.8 Four-box analysis for flexible protection.

Summarizing, the design challenge presented here seeks to develop cost-efficient protective materials for personnel applications that enable flexibility without a significant increment of weight.

3.5.2 Search

By using Asknature.com and scientific databases a large group of biological models appeared, including animals covered with thick skins like rhinoceros, mollusks covered with tough materials like nacre, and hard exoskeletons like those protecting crustaceans. However, since one of the main challenges here was to provide protection while enabling flexibility, the group of biological models was limited to animals protected with segmented natural armor (i.e., scales and osteoderms). To obtain these results, relevant keywords were used, including: "armor", "protection", "flexibility", "carapace", "exoskeleton", "shell", "scales", and "osteoderms".

As described in Section 2.1, animals protected with segmented natural armor are characterized by being protected by hard units (i.e., scales or osteoderms) linked together by flexible fibers. While hard units provide local protection against predatory loads, flexible fibers enable relative motion between hard units, generating overall flexibility. The protective systems of Arapaimas, Alligator gars, and Pangolins are good examples of scaled arrangements, while Alligators, Leatherback Turtles, and Armadillos comprise a good example of animals protected with osteoderms (see Section 2.1).

3.5.3 Simplify

As discussed in Chapter 2, protection systems based on scales and osteoderms exhibit similar functional principles. Despite their differences these systems present segmented arrangements, are organized in hierarchical structures, and most of them exhibit graded

mineralization. Since these concepts were already exposed in Section 2.1 a brief description of them is presented here.

By distributing predatory loads (generated by predator's claws and teeth) over broader areas, the hard units found in these arrangements reduce stress concentration, and thus less damage is caused in the underlying tissue. On the other hand, segmentation provides enhanced flexibility when compared with monolithic structures, since the flexible tissues connecting hard units enable relative motion between them. A graphical representation of this functional principle is shown in Figure 3.9.

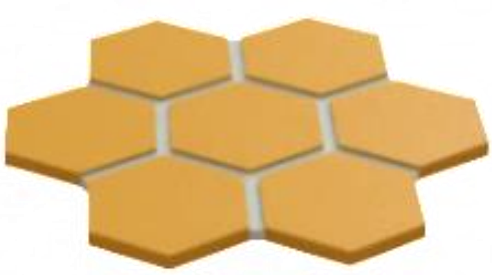

Figure 3.9 Graphical representation of a segmented arrangement.

A hierarchical structure is a common characteristic among biological materials. This structural configuration exhibit organized structures that range from the atomic to the macroscale assembled following a hierarchical pattern. Specifically, the hierarchical structure of elasmoid scales (like those exhibited by *Arapaima gigas)* consists of micrometric collagen fibers reinforced with nanoscopic mineral crystals. Fibers are arranged in unidirectional layers that are in turn organized in a cross-ply configuration that exhibits a higher degree of mineral content towards the outermost layers of the scale (see

Figure 3.10). At millimeter scales, this cross-ply arrangement comprises the Elasmodine, which is covered with a highly mineralized external layer termed Limiting layer.

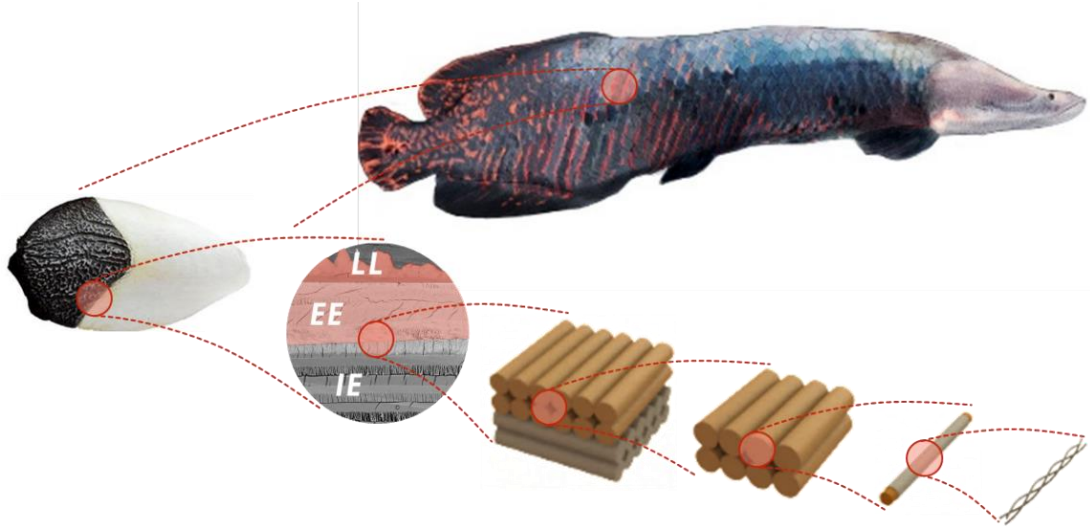

Figure 3.10 Graphical representation of the hierarchical structure of Arapaima scales. LL: limiting layer, EE: external elasmodine, and IE: internal elasmodine.

Hierarchical structures provide enhanced protection in puncture tolerant natural systems like scales and osteoderms since these configurations allow simultaneous activation of energy dissipation mechanisms at multiple length scales.

The last functional principle observed in segmented natural armor is graded mineralization. Specifically, elasmoid scales present a higher degree of mineral content towards the outermost layers of the scale, providing a hard-external surface bound to a tough underlying substrate (see Figure 3.11). This configuration provides efficient protection without a significant increment of weight, since denser minerals are concentrated in few external layers instead of being equally concentrated along the complete cross-section of the scale.

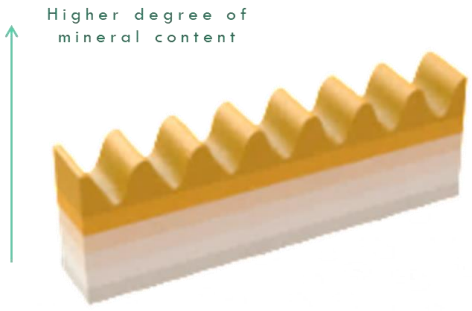

Figure 3.11 Graphical representation of the graded mineralization present in elasmoid scales cross-section.

As shown, the three functional principles identified in segmented natural protection are associated with specific requirements of the defined problem: segmentation provides flexibility, hierarchical structures provide energy dissipation at multiple length scales (thus enhanced protection), and graded mineralization enables efficient protection without a significant increment of weight.

3.5.4 Conceptualize

To include the identified functional principles into synthetic configurations many unsatisfactory ideas emerged during the development of this doctoral work. For example, to include segmentation into impact tolerant materials it was proposed to fabricate individual hexagonal segments to be subsequently assembled through flexible substrates. Likewise, to introduce graded mineralization, it was proposed to bond hard ceramic plates with a compliant substrate comprised of laminar composite materials. However, most of these ideas were abandoned through the design process because they were not compatible with industrial scalability, or because they would have significantly increased the weight

or the cost of the materials. The final conceptual solutions presented below are the result of several years of hard work and were finally selected to be fabricated and tested due to its potential industrial scalability.

To generate segmentation in synthetic materials, this work proposed to use a manufacturing process typically used in bioinspired segmented armor: laser engraving (see Section 2.2.2). On the other hand, unidirectional organic laminar composites were used to introduce synthetic hierarchy. Finally, to generate artificial graded mineralization, this work proposed a novel technic called bioinspired nano-mineralization, which consists of adding nanominerals into the outermost layers of a laminar composite. One of the main advantages of these conceptual solutions is their potential to be simultaneously implemented, providing typically divergent properties into synthetic materials (i.e., flexibility, protection, and lightweight). The fabrication and testing of these conceptual solutions do not belong exclusively to the conceptualization domain; therefore, these are presented in Chapters 4 and 5.

3.6 Concluding remarks

After millions of years of evolution, natural systems have inspired engineers to design and fabricate novel materials and devices with enhanced attributes and properties. This discipline is known as biomimetics and is characterized by moving across two different domains of knowledge: biology and engineering. This multidisciplinary nature is a fertile scenario for the emergence of novel design concepts. However, language differences between engineers and biologists generate implementation difficulties for bioinspired design. Aiming to close the gap between these two domains of knowledge, multiple design

methodologies for bioinspired design has emerged in the last decades, however, most of them are hardly implemented in industrial scenarios due to their complex and overwhelming routes.

This work proposes that instead of using complex methodologies, simplification is key for biomimetics popularization. Current successful bioinspired developments such as Velcro and Fastskin support that idea. Consequently, this work proposed a simplified methodology for bioinspired design comprised of the following four steps:

1) Define.
2) Search.
3) Simplify.
4) Conceptualize.

To test the proposed methodology in a real design challenge, the methodology was used to develop bioinspired design concepts for flexible protection obtaining simple ideas that can be replicated using current manufacturing technics. On one hand, laser engraving was proposed to introduce superficial segmentation within synthetic materials aiming to obtain enhanced flexibility. On the other hand, the use of laminar composites was proposed to introduce new levels of hierarchy in synthetic arrangements. Finally, by using the proposed simplified methodology, a novel manufacturing process emerged: bioinspired nano-mineralization. This new technic allows mimicking the graded mineralization present in fish scales.

Chapter 4: Bioinspired nano mineralization

This Chapter describes a novel technic termed as bioinspired nano-mineralization. By using *Arapaima gigas* fish scales as inspiration, nano-scale mineral reinforcements (e.g., Al_2O_3 and TiN) were incorporated into laminar organic fibrous composites (UHMWPE) to develop a system that emulates the natural graded mineralization present in the scales. New orders of hierarchy were introduced within the structure of this impact tolerant system triggering new energy dissipation mechanisms at the nanoscale. Using this strategy, a new generation of composites with five orders of hierarchy was developed rendering a considerable enhancement of energy absorption without a significant increase in weight.

As discussed in Chapter 2, Arapaima fish have elasmoid scales, which provide protection especially against piranha attacks. The *Arapaima gigas* is a species of arapaima that is native to the Amazon River basin of South America and is among the world's largest freshwater fish. It is covered by scales with lengths between 5 - 7 cm and average widths of ~ 4 cm (Lin et al. 2011). The Limiting Layer (LL) of its scales is about 600 μm in thickness, while the elasmodine can be as thick as 1000 μm. Unlike most other fish, the lamellae of the elasmodine are arranged with a stacking sequence of approximately 0°/90°, which is equivalent to a cross-ply orthogonal laminate structure (Murcia et al. 2017). The ply thickness ranges from 30 to 60 μm (Murcia et al. 2017; Yang et al. 2014). The constitutive fibers of each lamellae have a diameter of approximately 1 μm and these in turn consist of a large number of fibrils of smaller diameter (~100 nm) (Yang et al. 2014). The mineral structure within the layer of these scales was recently detailed and consists of platelets with a thickness of ~50 nm and diameters of ~500 nm (Lin et al. 2011; M. A.

Meyers et al. 2012). Overall, the microstructure of the Arapaima gigas scales exhibits six orders of hierarchy (Figure 4.1a).

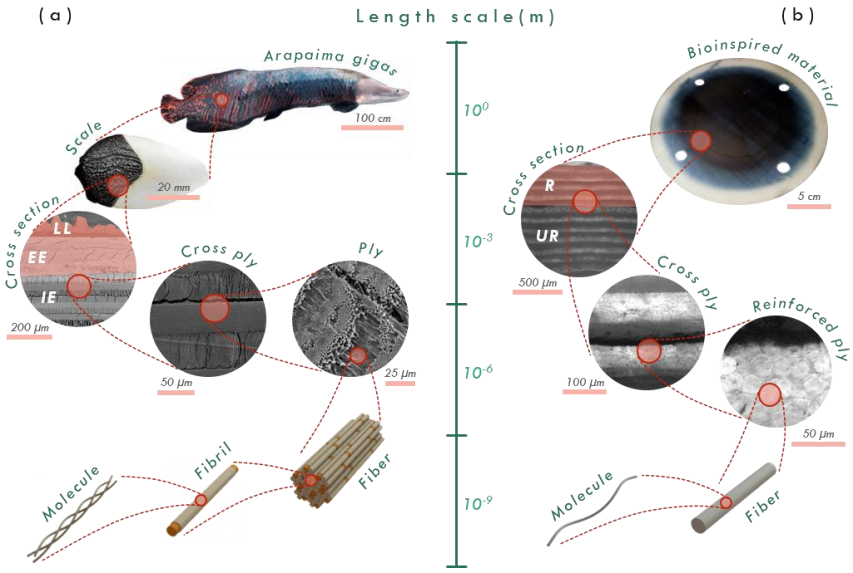

Figure 4.1 Hierarchical structure of Arapaima gigas scale and bioinspired mineralized composite, from the macro (100 m) to the atomic scale (10-9 m). Coloring represents a higher degree of mineralization. (a) Hierarchical structure of Arapaima scales, shown from top to bottom: Arapaima gigas fish, an elasmoid scale, a cross-section of the scale, collagen fibers arranged in a cross-ply configuration, a ply of unidirectional fibers, a mineralized collagen fiber with colored dots representing hydroxyapatite, a mineralized collagen fibril with colored dots representing hydroxyapatite, and the tropocollagen structure of the collagen molecule. (b) Hierarchical structure of bioinspired composites, showing from top to bottom: a plate of bioinspired material, the cross-section of the laminate showing graded mineralization (R, Reinforced and UR, Un-reinforced), UHMWPE fibers arranged in a cross-ply configuration with a nano-mineralized layer, two plies of UHMWPE fibers reinforced with a layer of nano-mineralization, a UHMWPE fiber and, a UHMWPE molecule.

4.1 Materials and method

Here we propose a material system inspired by the structure of Arapaima gigas scales. The foundation is a laminated composite of unidirectional plies of ultra-high molecular

weight polyethylene (UHMWPE) fibers within a rubber-based matrix. The laminate possesses a cross-ply arrangement similar to the 0°/90° ply configuration of Arapaima scales (Murcia et al. 2017). These composites are widely used in the armor industry under brands such as Spectra® and Dyneema®. Analogous to the mineral reinforcement of scales, we introduce nano-scale mineral reinforcements between the exterior-most layers of the laminate to increase the strength and energy absorption, without significantly increasing the weight of the material. The structure of this newly constructed material exhibits principles that are consistent with those of the *Arapaima gigas* scales (Figure 4.1b).

The laminates were comprised of eight layers of Dyneema® HB50, consolidated into a plate by thermo-pressing. Selected properties of Dyneema® HB50 and Dyneema® fibers are shown in Table 4.1. Each layer of Dyneema® HB50 consisted of four plies of unidirectional fibers cross-plied at 90° to each other. The laminates were pressed at 100 bar at a temperature of 125 °C for 35 minutes and then removed from pressure once the temperature was below 60°C, following material's supplier recommendations. For repetition, 5 samples of each design were fabricated and tested.

Table 4.1 Selected properties of Dyneema HB50 and Dyneema fibers. Information obtained from suppliers' data sheets (Dyneema® 2008, 2014).

HB50	Dyneema fibers		
Areal density (g/m^2)	Axial tensile modulus (GPa)	Transverse modulus (GPa)	Elongation at break (%)
226 - 240	52 - 132	3	3 - 4

To compare the mechanical performance and structural differences of the bioinspired materials, three different types of composites were fabricated: *i*) Unreinforced laminates of the UHMWPE composite, *ii*) Reinforced laminates with Aluminium Oxide (Al_2O_3) nanoparticles, and *iii*) Reinforced laminates with Titanium Nitride (TiN) nanocoating. Each sample consisted of a disc-shaped plate with a 200 mm diameter and ~2 mm of thickness (see Figure 4.2a).

Two different manufacturing strategies were adopted to introduce the nano reinforcements into the laminates. A nano-spray process was used to deposit spherical nano-particles between the laminate plies, while Radio Frequency Magnetron Sputtering was used to introduce the nano-coatings.

4.1.1 Aluminium Oxide reinforced laminates

The nano-spray process for introducing the Al_2O_3 nanoparticles reinforcement consisted of spraying three of the eight layers of the laminate with a colloidal suspension. These reinforced layers were stacked successively towards the external face of the laminate, combined with five non-reinforced layers, followed by thermo-pressing (see Figure 4.2b). After thermo-pressing, the stacking sequence of the laminate exhibited two different regions along the cross-section, which resembled the elasmodine structure of Arapaima scales. Specifically, the laminate consisted of a mineralized external region (i.e. EE), and a non-mineralized basal region (i.e. IE) (Sherman et al. 2017).

In the manufacture of Al_2O_3 reinforced laminates, liquid polyurethane (PU) was mixed with Al_2O_3 nanoparticles (~500 nm in diameter, MSESUPPLIES). The mixture was prepared in the following weight proportions: PU 41.7%, solvent 21%, catalyst 26.9% and Al_2O_3

particles 10.4%. The mixture of nanoparticles was applied by using a paint gun in two layers of homogeneous thickness, reaching approximately 500 mm. Three of the eight layers forming the bioinspired laminate were coated with this mixture between 1 and 10 minutes after adding the catalyst. The coated layers were left to dry for 24 hours at room temperature before consolidating into a laminate through thermo-pressing.

4.1.2 Titanium Nitride reinforced laminates

Titanium Nitride (TiN) layers were produced by a high vacuum Radio Frequency Magnetron Sputtering equipment (H2 Intecovamex) configured with a cubic stainless-steel vacuum chamber (300x300x300 mm). The distance substrate - target was 100 mm. High purity (99.995%) Titanium discs were used as the magnetron-sputtering targets. The sputtering process was developed at 5 mTorr of pressure in atmosphere of Argon (90%) and Nitrogen (10%) during 70 minutes at 150 Watts of Radio Frequency Power.

To manufacture the TiN reinforced laminates the three outermost layers of the composite were coated before thermo-pressing with a thin layer of TiN (~300 nm in thickness) using radio frequency magnetron sputtering. Thereafter, the reinforced and unreinforced layers were stacked and thermo-pressed with the same two-region configuration described for Al_2O_3 reinforced laminates (see figure 4.2b).

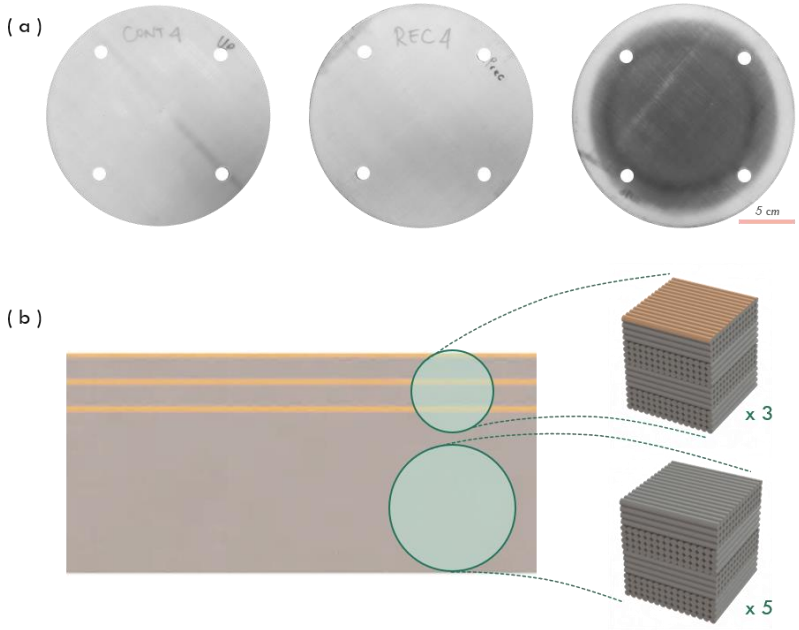

Figure 4.2 Bioinspired impact tolerant materials. (a) *Pictures of bioinspired samples. Shown from left to right: unreinforced laminate, laminate reinforced with Al2O3 nanoparticles, and laminate reinforced with TiN nanocoating. (b) Schematic mineral distribution of reinforced materials. Coloring represents mineralization. The three outermost layers of Dyneema® HB50 were reinforced with minerals (i.e., Al2O3 nanoparticles or TiN nanocoating) while the five inner layers were unreinforced.*

4.1.3 Impact tests

Impact tests were performed on the manufactured samples by using a fully instrumented TA Electro Force 3300 equipment with a loading rate of 2 m/s. A custom clamping was used to hold the laminates in place during impact, in which laminates were fixed through bolts, leaving 100 mm of free space for the laminate to deform. The clamping device was made of hardened steel (Figure 4.3a). The steel striker was made with a conical-spherical shape to allow a considerable energy transfer to the laminates tested (Figure 4.3a). The impact results were evaluated at 4 mm of deflection in all the tests to stay at a maximum of 0.5R of deformation, where R is the striker tip radius. Special care was taken to avoid

any slip of the samples during testing by using sandpaper between samples and clamping device.

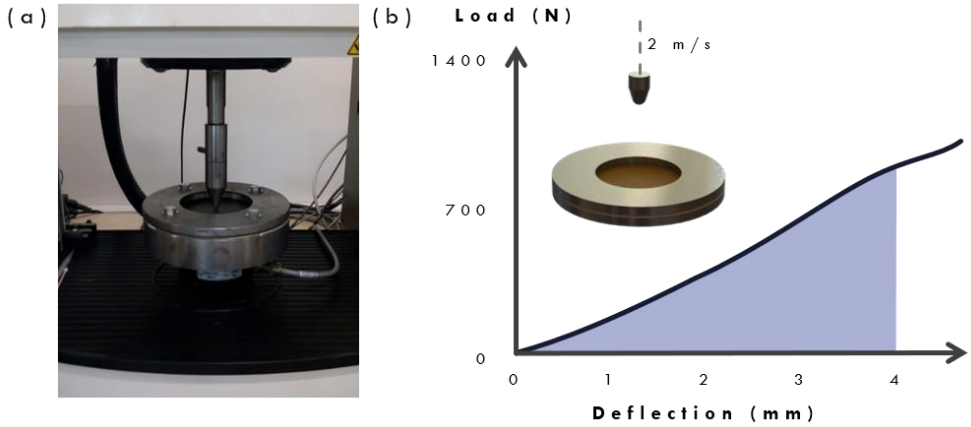

Figure 4.3 Impact test. (a) Impact test fixture showing clamping and striker. (b) Typical load-deflection response on an impact test. Mechanical strength is defined as the maximum impact load achieved at 4 mm of deflection, while energy absorption was defined as the area under the load-deflection curve from 0 to 4 mm of deflection.

A typical load-deflection impact response is shown in Figure 4.3b. Mechanical strength was considered here as the maximum impact load at 4 mm of deflection, stiffness was defined as the ratio between load and deflection at 4 mm of deflection, and the energy absorbed was defined as the area under the load-deflection curve once achieved 4 mm of deflection, as shown in Figure 4.3b. The choice of 4 mm of displacement to evaluate the energy absorbed by the tested samples ensured to have a constant speed of the striker up to this point. Soon after 4 mm the striker started to decelerate, reducing the impact speed. Further, after approximately 1 mm of displacement the deformation of the samples showed permanent deformation (plasticity), which was important as a measure of the energy absorbed by the samples. It is worth noting that none of the samples tested reached failure.

4.1.4 Microscopy tests

Small sections of the bioinspired laminates (about 2 mm in thickness) were embedded in cold-cured epoxy resin in order to inspect their microscopic characteristics. These sections were further ground with sandpaper with successive grit sizes of 120, 220,400, 600, 1000 and 1200, until having final thicknesses of the laminates of about 200 μm. Further polishing by means of red felt polishing cloths was performed using diamond particles of 6 μm, 3 μm, and 1 μm in size. Optical microscopy was then carried out on the samples using transmitted light by using an optical microscope (Axiovert 40 MAT, Carl Zeiss, NY). The same samples were further used for atomic force microscopy analysis. Images were obtained at standard conditions (T = 20 °C and R.H. = 50%) using an atomic force microscope (AFM; XE7, Park Systems Inc.). Commercial silicon AFM tips with diamond-like carbon (DLC) coating (TAP150, Budget Sensors) having a nominal stiffness k = 5 N/m and tip radius R = 25 nm were used in the phase non-contact mode.

4.2 Results and discussion

One of the main differences between the two typologies of reinforced laminates manufactured was the continuity of the reinforcing phase. While the Al_2O_3 particles consisted of discrete particles dispersed in a polyurethane matrix, the TiN nano-reinforcement was configured in a continuous layer as shown schematically in Figure 4.4. The dispersed reinforcement of Al_2O_3 is shown between the fiber plies in Figure 4.4a, and the continuous reinforcement of TiN is shown as a monolithic layer between fiber plies in

Figure 4.4d. Both of the reinforced laminate configurations possess a five-order hierarchical structure as shown in Figure 4.1b.

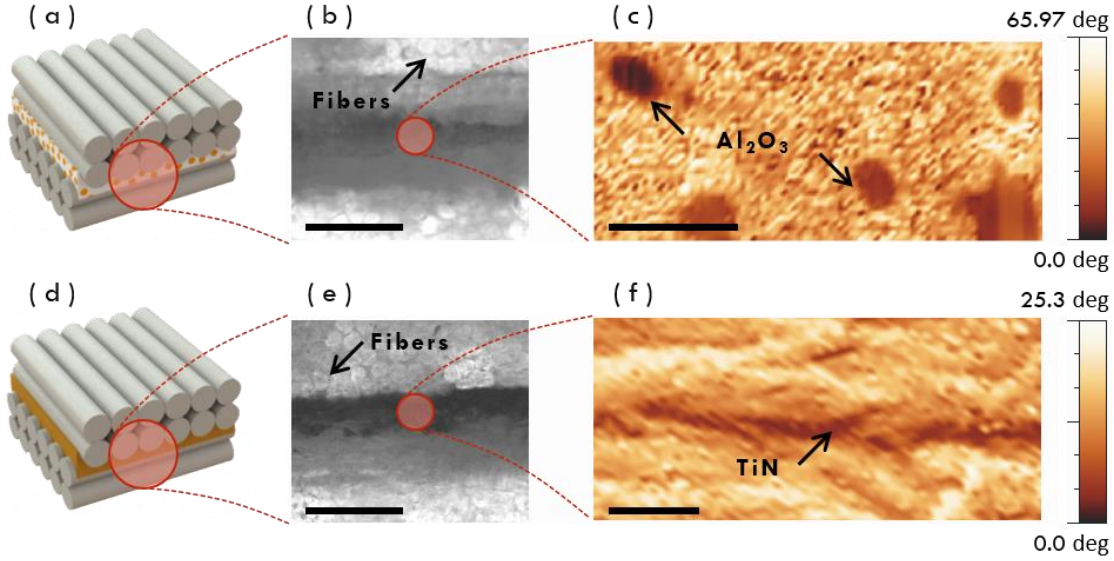

Figure 4.4 Micro and nanostructure of the bioinspired laminates. (a) scheme of cross-ply fibers reinforced with Aluminium Oxide (Al2O3) particles in a polyurethane matrix; (b) cross-section of a laminate reinforced with Al2O3 observed with optical microscopy using transmitted light, scale bar corresponds to 100 µm; (c) AFM non-contact phase image of a laminate reinforced with Al2O3 nanoparticles with a diameter of ~500nm, scale bar corresponds to 1 µm, Al2O3 nanoparticles are pointed by arrows; (d) scheme of cross-ply fibers reinforced with Titanium Nitride (TiN); (e) cross-section of a laminate reinforced with TiN observed through optical microscopy using transmitted light, scale bar corresponds to 100 µm; (f) AFM non-contact phase image of a laminate reinforced with TiN showing a TiN layer of ~300 nm, scale bar corresponds to 1 µm, TiN layer is pointed by an arrow.

4.2.1 Microscopy results

The microstructure of the bioinspired laminates is shown in Figures 4.4b and 4.4e, with light and dark alternating regions representing layers of fibers arranged in a cross-ply configuration. The fibers oriented perpendicular to the observer can be seen in the lighter

areas of the image, where circular individual UHMWPE fibers with a diameter of ~17 μm can be seen. The dark area towards the center of the images corresponds to one nano-mineralized layer. Figure 4.4c shows the structure of Al_2O_3 particles with diameters of ~500 nm dispersed in the polyurethane matrix, while Figure 4.4f shows the TiN nano-layer with a thickness of ~300 nm.

4.2.2 Impact results

Results of the impact tests show that both the Al_2O_3 and TiN nano-scale reinforcements increased the impact resistance of the bioinspired composites (Figure 4.5). While the unreinforced composites reached an average maximum load of approximately 915 N, the bioinspired composite reinforced with Al_2O_3 nano-particles reached an average maximum load of 1070 N, representing over 17% increase in impact load. On the other hand, the nano-reinforced TiN composites achieved an average maximum load of 1120 N, an increase of approximately 22% when compared with the unreinforced material.

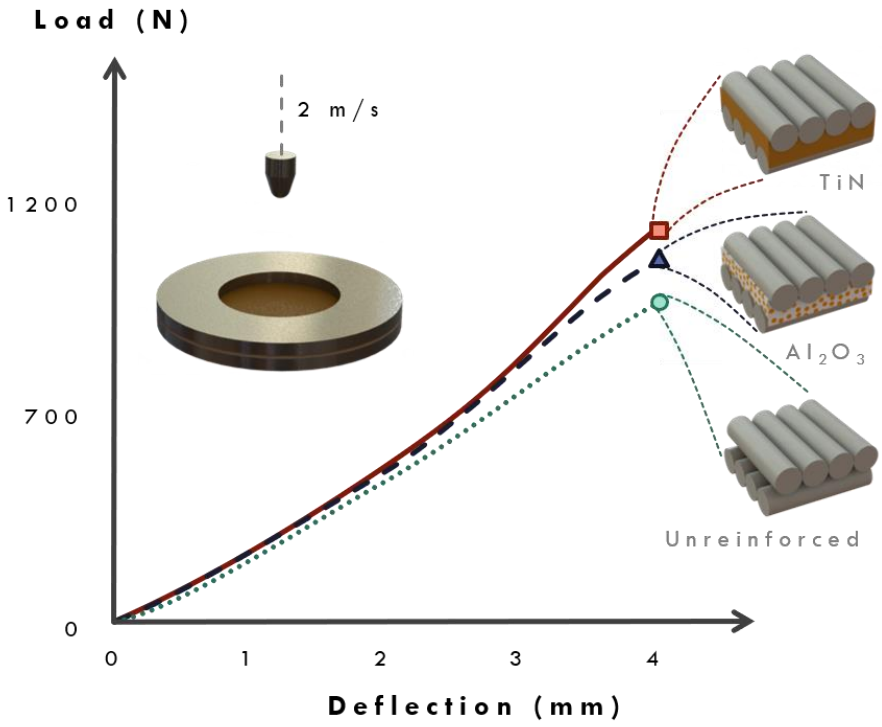

Figure 4.5 Load versus deflection response from the impact tests performed on the bioinspired and unreinforced materials. Colored areas with transparency represent the standard deviation of the measured responses for each type of material.

The differences in resistance to transverse deformation of the reinforced composites under impact loading are also reflected in their ability to absorb impact energy. Figure 4.6 shows the absorbed energy profiles for the materials, with respect to their stiffness. While the unreinforced material reached an average absorbed energy of 1.64 J with stiffness of roughly 230 N/mm, the laminate reinforced with Al_2O_3 reached an average absorbed energy of 1.87 J with a stiffness of 270 N/mm. That represents a 15% increase in absorbed energy with a 17% increment of stiffness for the Al_2O_3 reinforced materials. On the other hand, the TiN-reinforced materials achieved a 1.91 J of absorbed energy with a stiffness of 280 N/mm. When compared to the unreinforced materials, that represents a 17% increase

in energy absorbed and an 22% increment in stiffness. In demanding impact loading applications like aerospace, body armor and sports equipment, energy enhancements of these levels can render equivalent weight reductions. The statistical analyses showed that the differences in response between the three different composites were significant ($p \leq 0.05$). The post-hoc analysis showed that there were significant differences between the unreinforced and bioinspired composites, but no significant difference in performance between the Al_2O_3 and TiN reinforced composites (see Table 4.2).

Table 4.2 Dynamic testing results for reinforced and unreinforced samples, showing the mean (μ), standard deviation (σ), and coefficient of variation (CV) of the load, absorbed energy, and stiffness achieved by each sample configuration under impacts at 2 ms^{-1}. For repetition, five samples for each configuration were tested (N=5).

Sample (N=5)	Load (N)			Energy (mJ)			Stiffness (N/mm)		
	μ	σ	CV	μ	σ	CV	μ	σ	CV
Unreinforced	915.9	121.9	13%	1.636	0.107	7%	228.9	30.5	13%
Reinforced with Al_2O_3	1071.5	114.6	11%	1.872	0.116	6%	267.9	28.6	11%
Reinforced with TiN	1119.5	89.0	8%	1.911	0.069	4%	279.8	22.2	8%

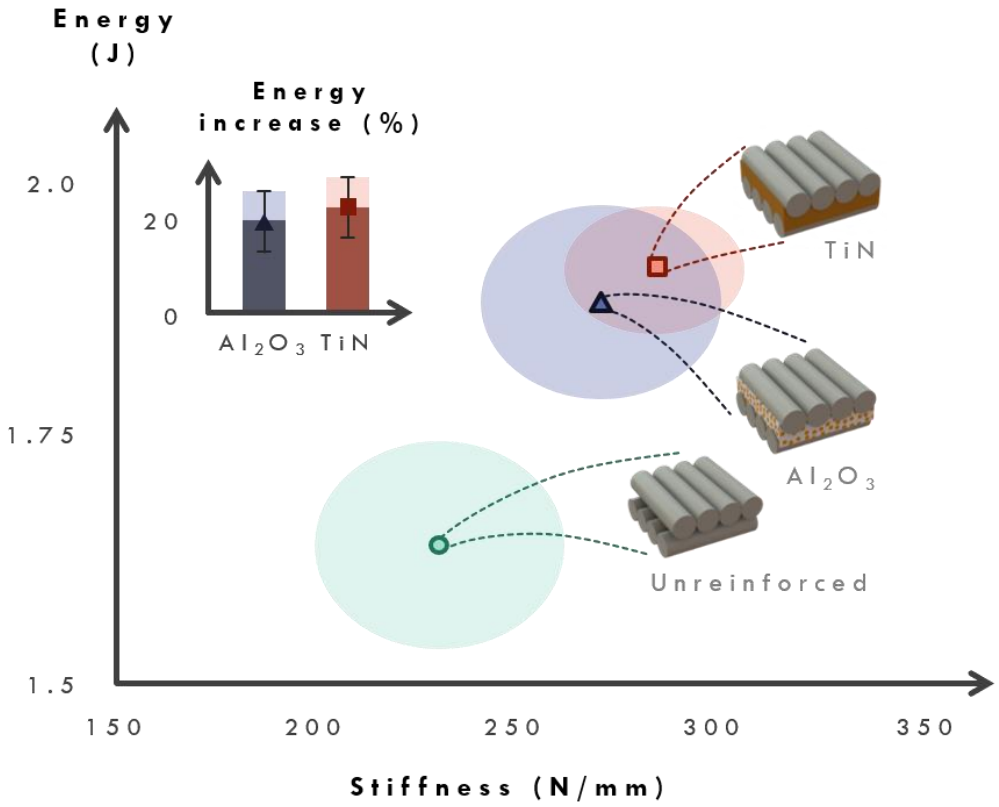

Figure 4.6 Absorbed energy versus stiffness of the bioinspired and unreinforced materials. The inset shows the percentage of energy increase of the reinforced materials (Al2O3 and TiN) in comparison to the unreinforced laminates. Colored areas with transparency represent the standard deviation of the measurements of each type of material.

4.2.3 Discussion

The introduction of hierarchical structures has recently been used to obtain extraordinary properties in synthetic materials (Gu, Takaffoli, and Buehler 2017). However, it is presently impossible to introduce hierarchy at length scales below the micro and macro scales by using technologies such as additive manufacturing or laser engraving. As such, nanotechnology appears to be the most viable option for introducing new levels of hierarchy in the development of synthetic materials. The bioinspired composites fabricated

in this study achieve five orders of hierarchy: *i*) the UHMWPE fibers; *ii*) a ply of unidirectional fibers; *iii*) a laminated layer of four cross-ply unidirectional plies; *iv*) three nano mineralized layers; and finally *v*) the bioinspired laminate with "graded" mineralization, similar to the EE and IE of fish scales (Figure 4.1). A sixth order of hierarchy could be achieved if the molecules of the polyethylene fibers were considered at the atomic scale.

Fish scales exhibit an interesting distribution of mineral content across their thickness. Arola et al. studied the mineral content of the outermost layer of the scale (LL) in different fish species (Arola et al. 2018). Regardless of species, the mineral content is maximum on the exterior surface of the LL, and then decreases to the LL/EE interface. The mineral content remains nearly constant in the EE and then undergoes an abrupt decrease to nearly zero in the IE [52]. In essence, the IE consists of plies of unidirectional collagen fibers without any mineral content. For the Arapaima scales, the volume fraction of apatite decreases from 60% to 40% over the thickness of the LL, remains nearly constant in the EE and then reduces to 0% within IE (Arola et al. 2018). Similarly, our bioinspired materials have highest mineral content towards the external layers of the composite due to the TiN and Al_2O_3 reinforcement. The volume fraction decreases to 0 % in the inner layers of the material, which mimics the distribution found in the EE and IE layers of elasmoid scales.

The mechanical properties of the bioinspired laminates are highly dependent on the properties of the reinforcement. The Young's modulus of Al_2O_3 and TiN is approximately 300 GPa and 600 GPa, respectively. Apart from Young's moduli, the difference in morphology between the two types of reinforcements is also important to the mechanical

responses. The Al_2O_3 particles were dispersed within a rubber-based matrix, serving as discontinuous reinforcements, while the TiN coatings formed a continuous layer of reinforcement, which is in direct contact with the UHMWPE fibers. The later configuration enhanced stress transfer between the reinforcements and fibers. It is worth noting that our bioinspired laminates have a minimal mineral content of approximately 1%, which is substantially lower than that of the Arapaima scales (40%). Achieving a mineral content of 40% in the external layers of the bioinspired laminates would double their weight in comparison to those without reinforcement. Clearly this would be problematic for industrial applications in aerospace and sports where weight reduction is always a priority.

The hierarchical approach involving the introduction of nano-scale reinforcements enabled the fabrication of high-strength composites with low-density. Both manners of reinforcement significantly increased the stiffness and energy absorption with minimal increase in weight (Figure 4.7). While the addition of Al_2O_3 reinforcements was accompanied by a 2.5% increase in weight, the TiN reinforcement caused an increase of approximately 0.15%. Both forms of the nano-scale reinforcements served as extremely thin layers of stiff reinforcements with no significant increase in weight. Nevertheless, both forms of reinforcement interacted with the UHMWPE fibers (Figure 4.6) and plies in a manner that improved the overall mechanical performance of the material.

A recent study concerning the deformation mechanisms of unreinforced UHMWPE composites under transverse impact reported that failure occurs in a progressive manner. Ply fracture begins at the interface between the striker and the composite and propagates to the rear of the laminate (Attwood et al. 2016). The failure process occurs through tensile failure of the plies by an indirect tension mechanism, wherein the transverse compression

stresses generate tensile stresses in-plane due to a mismatch in the properties between the alternating 0° and 90° plies. This process is accompanied by fiber sliding, which is evidenced by outward extruded fibers found in the cross-section of the impacted composites. This interaction occurs at both the ply and fiber levels, which ranges across three decades of length scale (1 μm to 1 mm). However, when nano-reinforcements are integrated into the laminates, interfacial friction between the plies limits the sliding and stretching of fibers, thereby improving the coupling between fibers. Thus, in the development of tensile stresses within the fibers through indirect tension, the increased friction spreads fiber recruitment in supporting the mechanical load. That process ultimately allows the stress to be distributed over wider areas, thus reducing damage. Certainly, the increased friction between fibers is a complementary mechanism of energy dissipation facilitated by the nano-scale reinforcements, which manifests as an increase in the mechanical performance of the reinforced materials at the macro scale.

Similar phenomena have been found in both natural and artificial systems. For instance, in fish scales, dehydration causes resistance to sliding between collagen fibers, which increases the elastic modulus and strength of dehydrated scales (Lin et al. 2011; Murcia et al. 2016). The stiffening mechanisms associated with this phenomenon have already been reported by Jiang et al (Jiang et al. 2020). Similarly, in synthetic systems such as liquid armor, the high-performance fabrics increase their mechanical properties via resistance to fiber sliding promoted by the introduction of Shear Thickening Fluids (STF) (Crouch 2019). STF are dense colloidal suspensions that can exhibit an abrupt increase in the viscosity with an adequate increase in shear rate or applied stresses. When used in protective applications, STF improve the performance of the fabrics, but their major contribution is not derived

from their shear thickening behavior. Rather, the solid particles increase the friction between fibers, which ultimately causes spreading of the load over wider areas (Ding et al. 2013; Gürgen, Kuşhan, and Li 2017; L. L. Sun, Xiong, and Xu 2013). Particle volume fraction and particle size are some of the characteristics that affect the performance of STFs. These factors could also affect our bioinspired materials. The lower limit of the particle volume fraction for the thickening behavior of colloidal suspensions depends on the material properties. It has been reported that the thickening behavior of STF is generally activated at a particle volume fraction exceeding 0.5 (Gürgen, Kuşhan, and Li 2017). In contrast, the volume fraction of Al_2O_3 particles in the present work was about 0.01, which is significantly lower than that stated to trigger the thickening behavior of the STF. Although impact tests show that this minimum volume fraction (0.01) can improve the energy absorption and stiffness of bioinspired laminates, future work investigating the effect of this volume fraction on the properties of the laminate is warranted, as this may open new opportunities for optimization.

An analysis of the relations between fibers and reinforcements for the natural and bioinspired materials show important similarities. The collagen fibers present in *Arapaima gigas* scales have a diameter of 1 μm with a mineral reinforcement consisting of platelets with a thickness of 50 nm (Lin et al. 2011; M. A. Meyers et al. 2012). On the other hand, the fibers present in our bioinspired laminates have a diameter of 17 μm accompanied by reinforcements of different sizes depending on the nano-mineralization strategy. The Al_2O_3 particles were approximately 500 nm diameter, and the TiN reinforced layer thicknesses were approximately 300 nm. The reinforcement/fiber (RF) ratio, defined as the ratio between particle diameter (or coating thickness), and fiber diameter, shows that the

Arapaima scales exhibit an RF ratio of 0.05. That value for the Al_2O_3 and TiN reinforced laminates is ~0.03 and ~0.02, respectively. Future studies that explore the importance of this ratio between the constituent units of bioinspired laminates and their effect on internal friction could lead to further improvements on mechanical properties.

Previous studies have shown that the stacking sequence of unidirectional fiber laminates can significantly affect the mechanical behavior of bioinspired composites. Hazzard et al. (Hazzard et al. 2017) showed that lamination patterns such as rotational, helicoidal or quasi-isotropic configurations can achieve superior mechanical behavior of thin Dyneema® panels under low-velocity impacts when compared with cross-ply arrangements. They suggested that the deformation mechanisms exhibited by cross-ply laminates were dominated by substantial in-plane shear with limited load transfer from primary fibers, which is an energy dissipation mechanism exhibited at the microscale (1 μm to 1 mm). The load transfer between fibers could be maximized by introducing nano-scale reinforcements following the strategy applied here. Considering that the laminates in this work were inspired by the cross-ply patterns in Arapaima scales (Murcia et al. 2017), further work could consider the combined effect of nano reinforcements and varying lamination patterns on the mechanical properties of the materials.

One of the prime aims of this work was to develop strategies for manufacturing hierarchical low weight energy absorption materials that could be easily adopted in the industry. The effect of the manufacturing process on energy and weight variations can be analyzed if a figure of merit relating energy absorbed, density and cost is used, as shown in Figure 4.7. Here, an increased value will represent low weight and low cost with increased energy absorption. According to this ranking, the addition of nanoparticles

stands out as a viable option for industrial scaling. Radio frequency magnetron sputtering increases the cost about 17 times in comparison to the unreinforced material, whereas the production cost of the nanoparticle reinforcements results in just about 1.3% increase. Given that no significant differences were found in the impact resistance between the two bioinspired materials, introducing reinforcements by nano-spray coating is considered the best option to be industrially scaled.

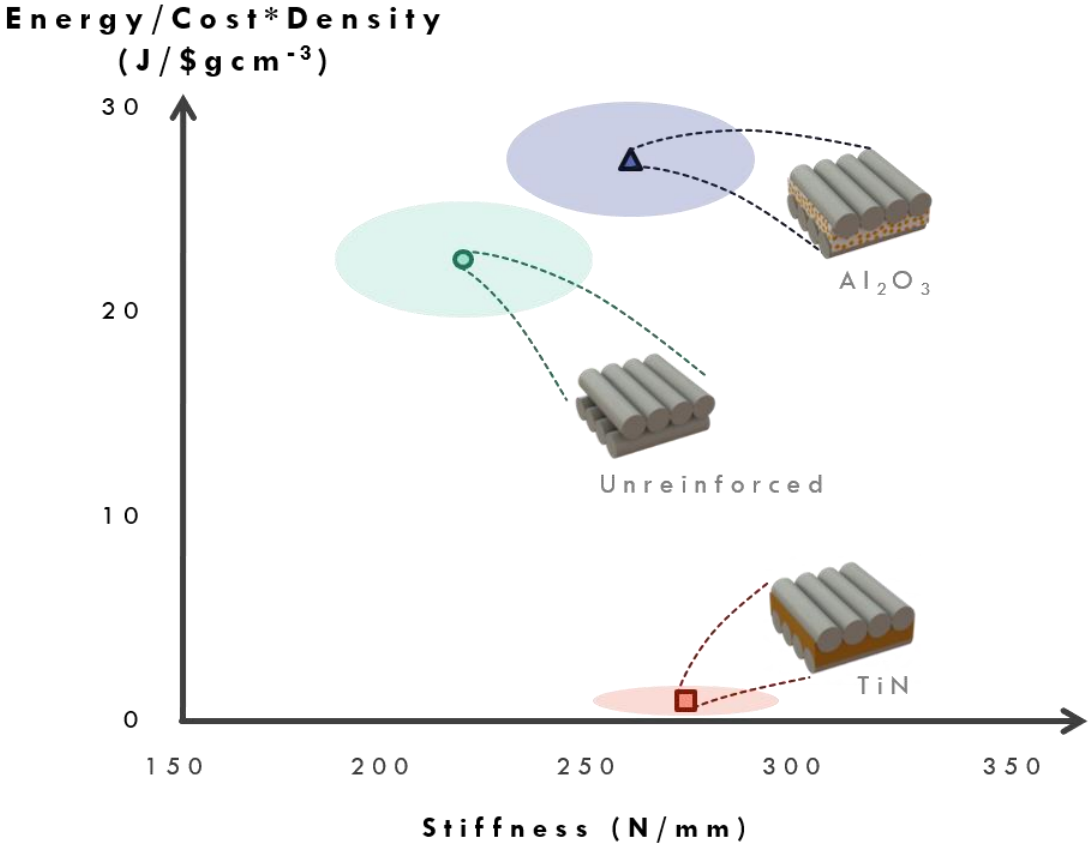

*Figure 4.7 Figure of merit representing materials performance accounting for energy absorption, weight and manufacturing cost (Energy/Cost*Density) as a function of the stiffness for the bioinspired and unreinforced composites. Colored areas with transparency represent the standard deviation of the measurements for each type of material.*

4.3 Concluding remarks

By using a novel fabrication strategy called bioinspired nano mineralization it was able to mimic the graded mineralization exhibited by Arapaima scales, with a variation in the mineral content from the top to the bottom of the material. By using two different nano mineralization strategies (i.e., Al_2O_3 nanoparticles and TiN nanocoating) into a laminar organic fibrous composite, three different sample typologies were obtained: *i)* unreinforced, *ii)* reinforced with Al_2O_3, and *iii)* reinforced with TiN. Dynamic tests revealed that the impact resistance of the reinforced materials was increased significantly with respect to the non-reinforced materials, with a 15% to 17% increase in absorbed energy for materials reinforced with Al_2O_3 and TiN respectively. Remarkably, this enhancement in impact performance was obtained with a negligible increase in the weight (i.e., less than 2,5 % in Al_2O_3-reinfoced materials and barely 0,15 % in TiN-reinforced materials). The microscopy analysis suggested that the enhanced impact performance resulted from a new energy dissipation mechanism at the nanoscale. This mechanism involves increased friction between the fibrous layers of the laminate through interfacial nano-scale reinforcements. Remarkably, the Al_2O_3-based mineralization strategy can be industrially scaled up due to their low added costs. Therefore, this strategy for developing bioinspired hierarchical materials may bring the benefits of biomimetics to the next generation of light-weight, cost-efficient, impact-tolerant, high-performance protective materials.

Chapter 5: Protecto-flexible impact tolerant materials

Besides the bioinspired mineralization described in Chapter 4, other biomimetic concepts were obtained through the use of the simplified methodology for bioinspired design (i.e., segmentation). By introducing segmentation into nano mineralized laminate composites, it was possible to increase the impact energy absorption in desired areas of the material while having enhanced flexibility in regions requiring relative movements. Further, the effect of different degrees of structural hierarchy was analyzed as well as how these improve protection and flexibility based on the corresponding energy dissipation mechanisms activated at each of these levels. Finally, a bullet-proof protecto-flexible prototype was manufactured and tested. The ballistic tests suggested, that under real stringent conditions, the system is capable of absorbing high levels of energy while remaining flexible enough to allow movement to the user.

As previously discussed, Arapaimas are covered with elasmoid scales, which provide protection especially against piranha attacks. These scales are characterized by exhibiting hierarchical structures and graded mineralization (see Chapter 2, 3 and 4). Unlike most other fish, the lamellae of the elasmodine are arranged with a stacking sequence of approximately 0°/90°, which is equivalent to a cross-ply orthogonal laminate structure (see Figure 5.1a). Armadillos, unlike fish, have a protective bony armor composed of osteoderms consisting of hard hexagonal or triangular tiles having a structure and composition similar to that of bone (see Figure 5.1c). These osteoderms are connected by

flexible collagen fibers, conferring flexibility to the system at the macroscale. These bony plates allow load distribution over broader areas, reducing the energy transfer of predatory bites to the underlying soft tissues (Martini, Balit, and Barthelat 2017; Yang, Chen, et al. 2013).

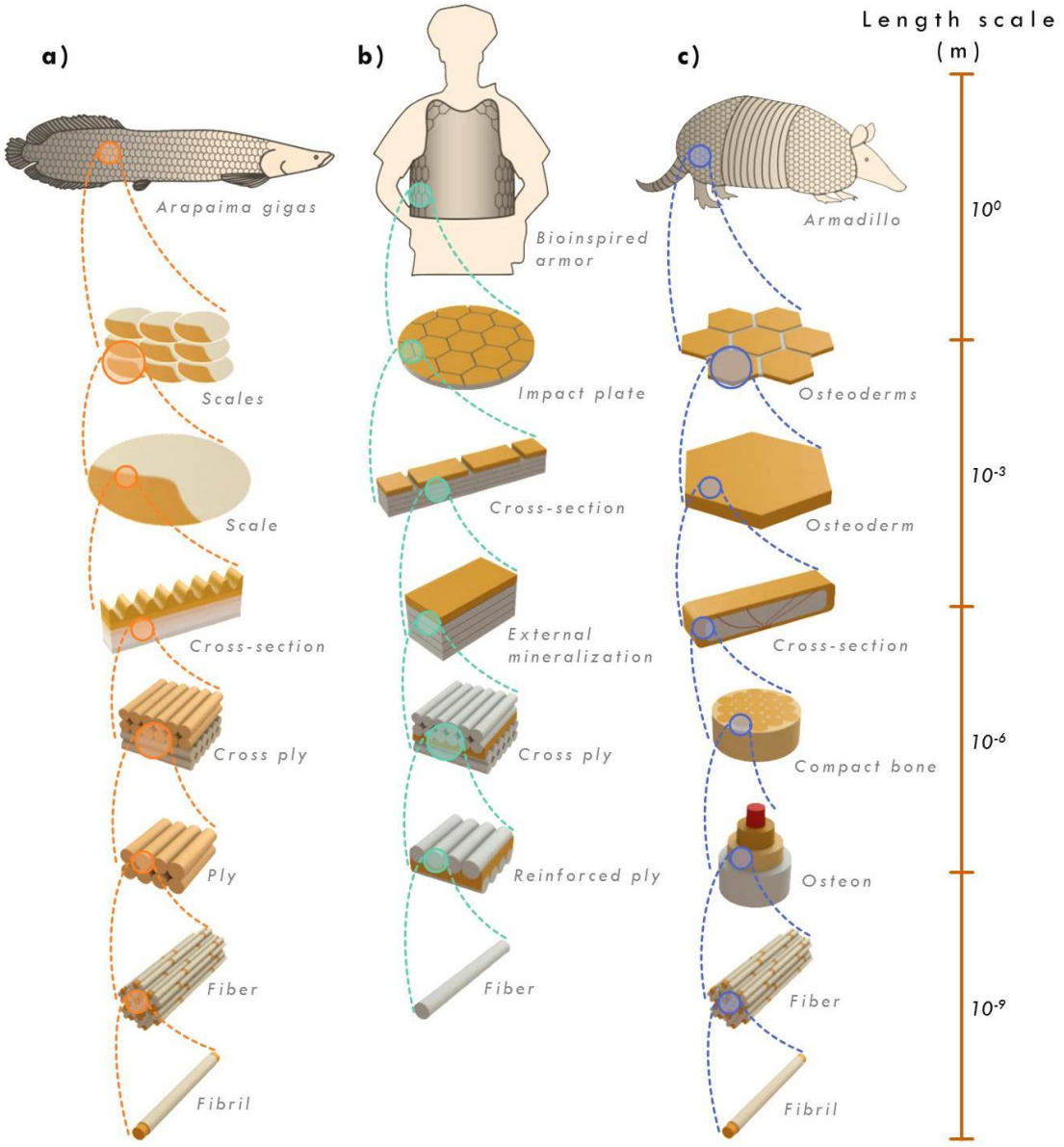

Figure 5.1 Hierarchical structure of Arapaima Gigas scales, bioinspired protecto-flexible armor, and Armadillo osteoderms from the macroscale (100 m) to the nanoscale (10-9 m). a) Hierarchical structure of Arapaima scales, shown from top to bottom: Arapaima gigas fish, an overlapping arrangement of scales, an

elasmoid scale, a cross-section of the scale, collagen fibers arranged in a cross ply configuration, a ply of unidirectional fibers, a mineralized collagen fiber with colored dots representing hydroxyapatite, and a mineralized collagen fibril with colored dots representing hydroxyapatite; b) Hierarchical structure of bioinspired armor, showing from top to bottom: a user wearing a bullet-proof insert, a plate of bioinspired protecto-flexible material, the cross-section of the laminate showing an engraved surface, a cross section of the laminate showing a graded mineralization, UHMWPE fibers arranged in a cross-ply configuration with a nano mineralized layer, two plies of UHMWPE fibers reinforced with a layer of nano-mineralization, and a UHMWPE fiber; c) Hierarchical structure of Armadillo osteoderms, shown from top to bottom: an Armadillo, a group of juxtaposed osteoderms bonded by collagen fibers, an isolated osteoderm, a cross section of a vascularized osteoderm showing its sandwich-like structure, the structure of compact bone, an osteon, a mineralized collagen fiber with colored dots representing hydroxyapatite, and a mineralized collagen fibril with colored dots representing hydroxyapatite.

To investigate the effects of increasing structural hierarchical levels on the ability to absorb impact energy and its related flexibility, Ultra High Molecular Weight Polyethylene (UHMWPE) was used as the base material, manufactured in different configurations ranging from monolithic (e.g. one level of structural hierarchy *H-1*) up to six levels of structural hierarchy (*H-6*), as shown in Figure 13a. Disc-shaped samples with 200 mm in diameter were prepared to be tested under dynamic loading conditions. *H-1* samples consisted of monolithic UHMWPE plates with ~3 mm in thickness (see Figure 13a). This configuration was used as the reference material as there is no natural counterpart. Monolithic plates were engraved with hexagonal superficial patterns inspired by armadillo's armor (*H-2*). Here, the hexagonal engravings emulate osteoderms connected by collagen fibers, to allow increased flexibility to the system (Figure 5.2a). (Allison et al. 2013; Chen et al. 2011; Yang, Gludovatz, et al. 2013). *H-4* samples were prepared by using

a UHMWPE fiber-based cross-ply arrangement similar to the 0°/90° ply configuration of Arapaima scales, with ~2 mm of thickness. (Murcia et al. 2017) The four levels of hierarchy were composed of the polymeric fibers (*I*), a layer of unidirectional fibers (*II*), the cross-ply arrangement (*III*), and finally its consolidation within a rubber matrix to form a plate (*IV*) (Figure 5.2a). Two different sample arrangements were prepared to achieve *H-5*. First, *H-4* samples were engraved with armadillo's inspired hexagonal patterns, leading to enhanced flexibility and an extra level of hierarchy (*H-5H*), as shown in Figure 5.2a. Analogous to the layers of mineral reinforcement found on scales' elasmodine, nano-scale mineral reinforcements between the exterior-most layers of the *H-4* material were introduced, without significantly increasing its weight. The *H-5R* configuration exhibits principles that are consistent with those of the Arapaima gigas scales (see Figure 5.1 and 5.2a). Finally, *H-6* was obtained by combining bioinspired hexagonal engraving patterns and the bioinspired mineralization strategy followed on *H-5R* samples (Figure 5.2a). The structure of this newly constructed material resembles the geometrical patterns found in armadillo's osteoderms and the flexible impact tolerant configuration found on fish scales.

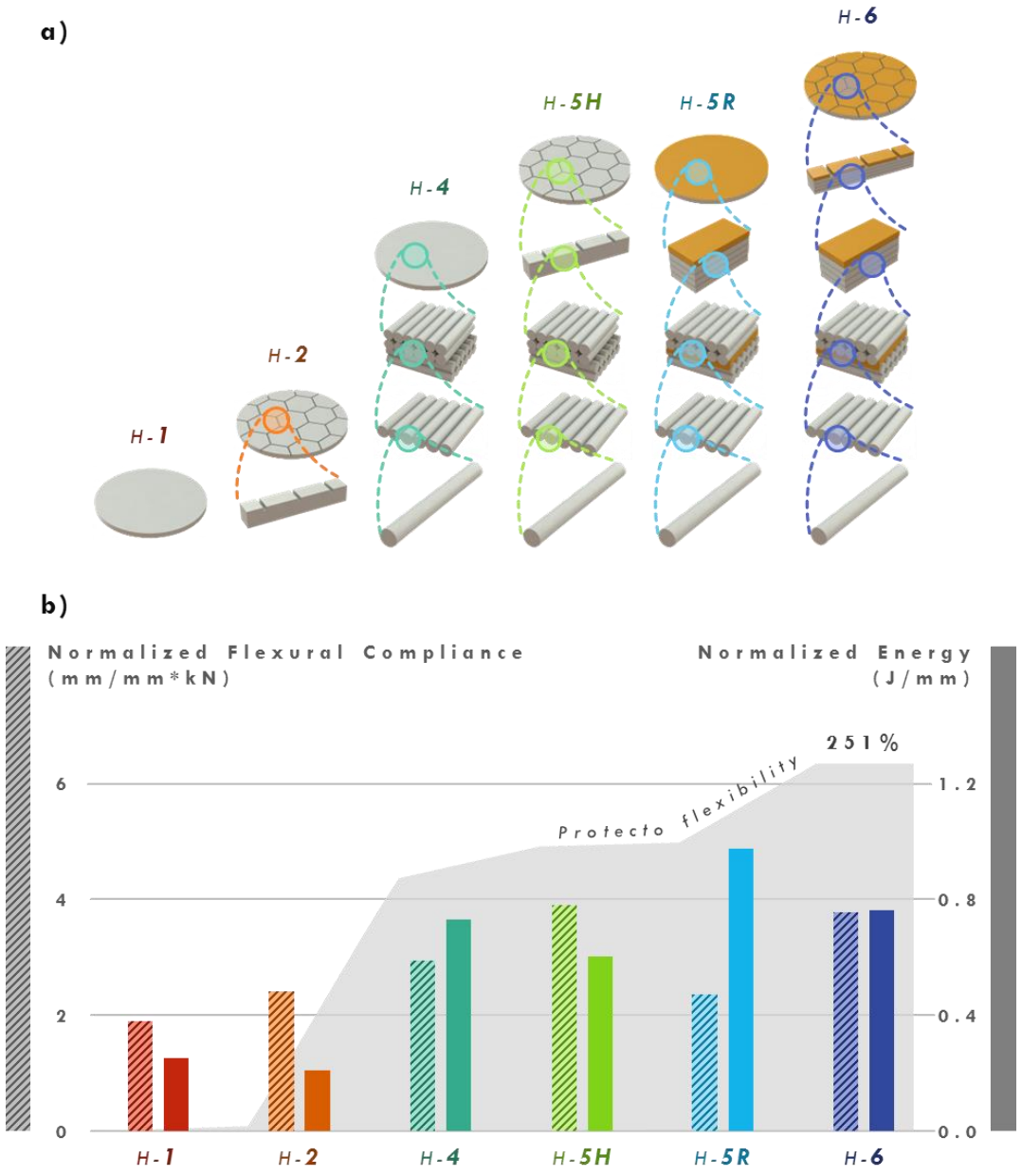

Figure 5.2 Samples with different hierarchical levels and their corresponding dynamic experimental results. a) Hierarchical structure of the different samples. From left to right: a monolithic sample consisting of one level of hierarchy (H-1); a sample with two levels of hierarchy (H-2) obtained by combining a monolithic sample with bioinspired engravings; a sample with four levels of hierarchy (H-4) consisting of polymeric fibers organized in unidirectional plies, stacked together in a cross-ply arrangement and consolidated into a plate within a rubber based matrix; a sample with five levels of hierarchy (H-5H) resulting by combining bioinspired engravings with H-4 samples; a sample with five levels of hierarchy (H-5R)

resulting by combining nano-mineralization in the external most layers of the laminate with H-4 samples; and, samples with six levels of hierarchy (H-6) resulting by combining bioinspired engraving with H-5R samples. b) Measured levels of flexural compliance, normalized energy and enhancement of protecto-flexibility. Stripped bars represent the measured flexural compliance corresponding to the left-hand axis; solid bars represent the measured normalized energy corresponding to the right-hand axis; and the shaded area represents the percentage increase in protecto-flexibility, as an estimate of the combined effect of energy (protection) and flexural compliance (flexibility).

5.1 Materials and methods

Samples for this work were divided in two groups: *i*) monolithic samples (*H-1* and *H-2*), and *ii*) laminated fiber-based samples (*H-4*, *H-5H*, *H-5R* and *H6*). Monolithic samples consisted of plates of Ultra High Molecular Weight Polyethylene (UHMWPE) with 3.175 mm of thickness. Laminated samples were based on UHMWPE fibers, which are widely used in the armor industry under brands such as Spectra® and Dyneema®. Laminated (H-4, H-5H, H-5R, and H6) and mineralized (H-5R and H-6) samples were fabricated as described in Chapter 4. However, here mineralization was only obtained through the use of Al_2O_3 nanoparticles (i.e. not TiN nanocoating). Engraved samples (*H-2*, *H-5H* and *H-6*) were carved using a laser engraving machine (Boye Laser, LS 1410) to configure hexagonal patterns with an edge length of 5.3 mm. For monolithic engraved samples (*H-2*) a cutting speed of 1000 mms^{-1} and machine power of 75% were used, obtaining an engraving pattern with a depth of ~1.1 mm and a width of 0.4 mm. The laminated samples (*H-5H* and *H-6)* were engraved using a cutting speed of 12000 mms^{-1} and machine power of 25%. The relatively high cutting speed and low power used here was intended to protect the laminated structure from the potential damage of fibers. However, to obtain the expected

depth, laser engravings were repeated 3 times for each laminate, obtaining an engraving pattern with a depth of ~1.1 mm and a width of 0.3 mm.

Dynamic impact tests at a rate of 2 ms^{-1} were performed on the samples to analyze their mechanical performance similar to those presented in Chapter 4. In particular, absorbed energy and flexural compliance exhibited by the samples were used as estimations of the protection and flexibility provided by the different configurations. Absorbed energy was defined as the area under load-deflection responses at a deflection of 4 mm, while flexural compliance was calculated as the ratio between deflection and load at the initial stages of deformation (e.g. ~1 mm) (see Figure 5.3).

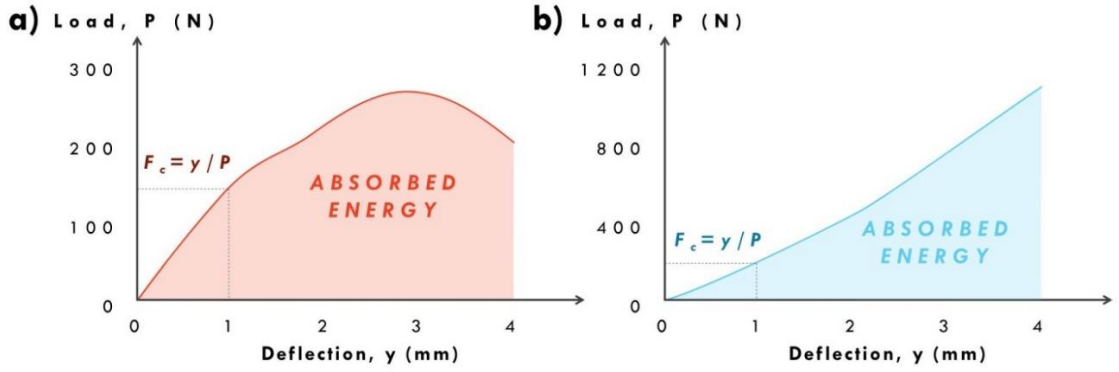

Figure 5.3 Typical load–deflection responses for a) monolithic and, b) laminated samples. Energy absorption was defined as the area under the load – deflection curve from 0 to 4 mm of deflection. Flexural compliance was estimated as ratio between deflection and load at 1mm of deflection.

The summary of all load-deflection responses and schematic diagrams showing the puncture behavior of the samples are shown in Figure 5.4. These diagrams are intended to show graphically the reduction of the tensile stress induced by puncture caused by engravings (*H-2*, *H-5H*, *H-6*), while showing the increased stiffness caused by bioinspired mineralization (*H-5R*, *H-6*). Specifically, the puncture diagram for the *H-6* samples

illustrates how the combination of bioinspired mineralization accompanied by superficial engravings promotes the distribution of localized loads over broader areas.

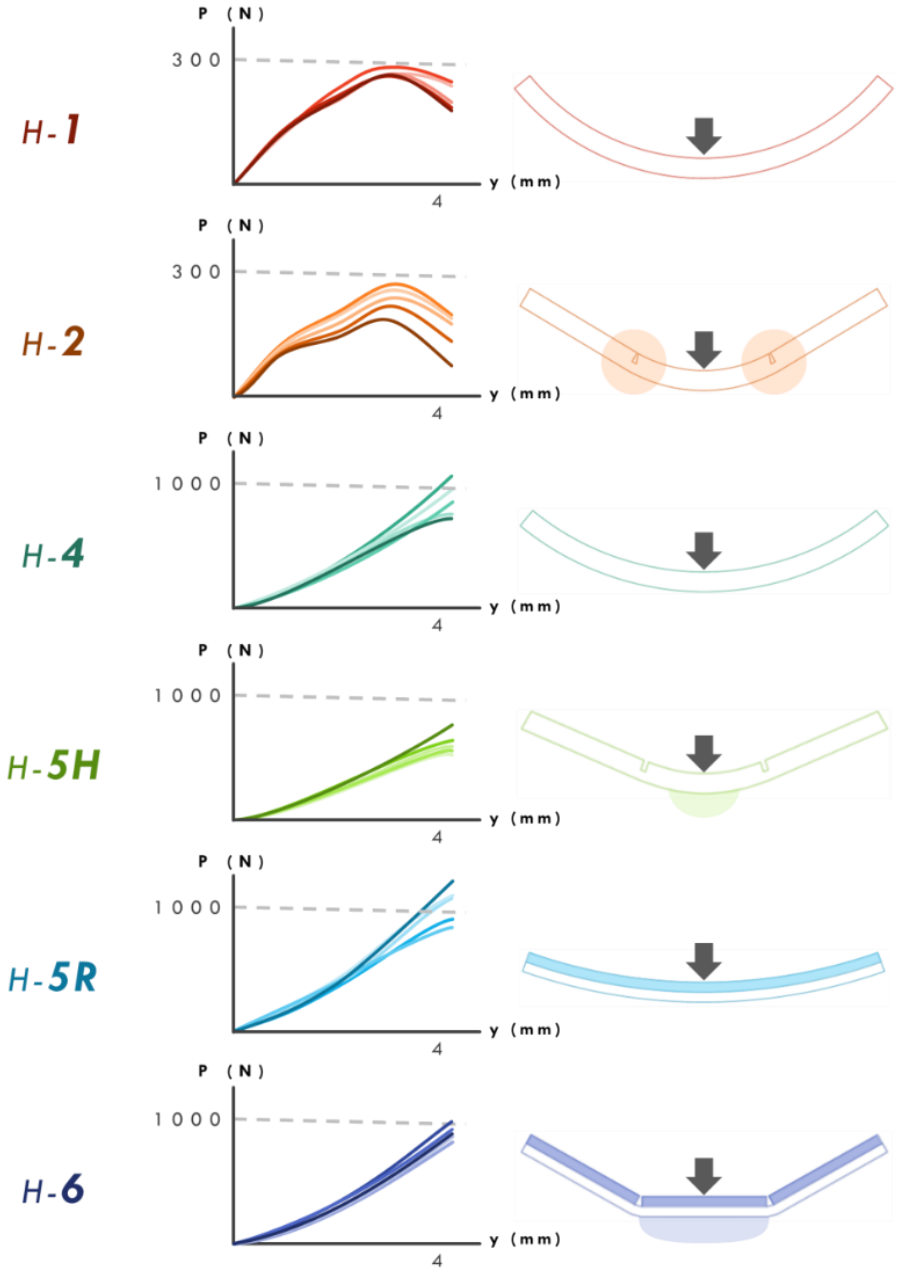

Figure 5.4 Typical load–deflection response for each sample typology and schematic diagrams representing the macroscopic puncture behavior of the samples

The simultaneous contribution of absorbed energy and flexural compliance was measured under the metric *protecto-flexibility*. This concept was initially proposed by Rudykh et al. as a measure of the ratio between indentation and bending stiffness in 3D printed scaled systems.(Rudykh, Ortiz, and Boyce 2015) In contrast, we adapt that metric here as a combined measure of absorbed energy (protection) and flexural compliance (flexibility), normalized by sample thickness (t), as:

$$Protecto\ flexibility = \frac{Absorbed\ Energy * Flexural\ compliance}{Sample\ thickness} \quad (1)$$

Measured normalized absorbed energy, flexural compliance and protecto-flexibility for the different structural hierarchical levels studied here are shown in Figure 5.2b and Table 5.1.

Ballistic tests on the prototype bulletproof material were performed by using a handgun with 9 mm ammunition. This ammunition possesses a muzzle velocity of 360 m/s and an impact energy of ~520 J. Ballistic samples consisted of 31 cm x 31 cm panels with *H-6* configuration. The samples were supported perpendicular to the shooter at a distance of 5 m and were fixed with straps to a substrate of ballistic clay (see Figure 5.5). Each ballistic sample was impacted twice at different positions. The panels were not penetrated through by the bullets, as shown in Figure 5.5b where the two bullets are shown in the impact zones. Notice that the bullet's impacts were close to the engravings performed in the panel without a considerable reduction in the response of the panel. It is worth mentioning that complete ballistic tests require estimation of muzzle velocities and projectile masses to

measure the ballistic limit (V_B) of the sample after several bullet impacts. However, this kind of test was out of the scope of our work and represent a future step towards the full development of the materials.

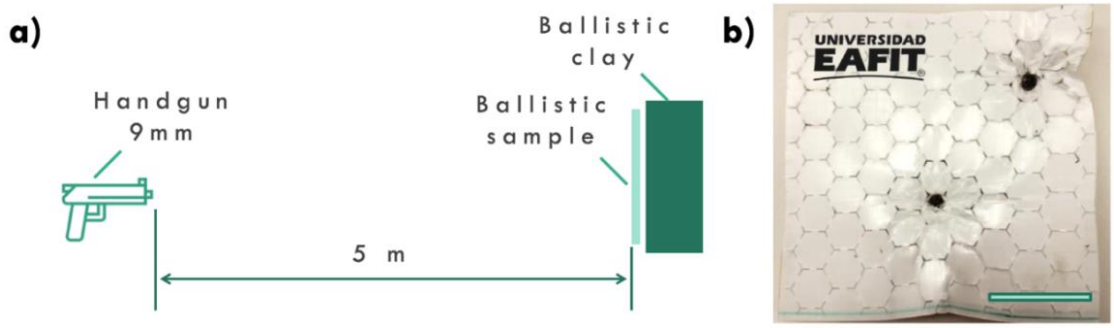

Figure 5.5 Ballistic tests on the prototype bullet-proof material. a) The ballistic test set up. b) Ballistic panel impacted with two 9 mm bullets, scale bar corresponds to 10 cm.

5.2 Results and discussion

Monolithic samples (*H-1*) exhibit high flexibility with moderate energy, while the inclusion of Armadillo's inspired hexagonal engravings (*H-2*) decreases the energy 16% with an increment of 20% in flexibility, leading to a combined increase of 1% on protecto-flexibility. The use of two extra levels of hierarchy (*H-4*), provided by the cross-ply arrangement of fibers, increases the energy 202% and the flexibility 45%, with an increase of protecto-flexibility of 172%. In-plane stresses are better supported by orthogonal fiber plies, leading to a considerable rise in absorbed energy in comparison to *H-1*. The inclusion of hexagonal engravings on *H-5H* leads to a reduction in absorbed energy with an enhancement of flexibility in comparison to *H-4*. However, the combined effect on protecto-flexibility shows important improvements of 8% in comparison to *H-4*, with a growing cumulative protecto-flexibility of 193%. The use of layers of mineral

reinforcement, similar to fish scales on *H-5R* allows an impressive increase in absorbed energy with a moderate reduction on flexibility. Recent studies have suggested that the increment in energy absorption induced by bioinspired nano-mineralization is highly associated with the interaction between fibers and nano-reinforcements. Particularly, Al_2O_3 nano-particles interact with the fibers by increasing interfacial friction between plies, causing a limited sliding and stretching of fibers and thus causing a better coupling between them. Therefore, in-plane stress induced by flexure spreads over broader number of fibers improving the absorbed energy of the *H-5R* samples. The inclusion of hexagonal engravings on *H-6* allows a superior combination between absorbed energy and flexibility, leading to an overall improvement of 251% on protecto-flexibility. This effect produced by superficial engravings is associated with the reduction of compressive stresses at the external-most layers, induced by flexure, which resembles the effect of superficial ridges in the external surface (LL) of fish scales (M. A. Meyers et al. 2012; Yang, Chen, et al. 2013). Despite the low volume fraction of nano-particles (i.e. 0.01) used to manufacture H-5R and H-6 samples (see Chapter 4), the improvement on the protecto-flexibility of these configurations is substantial. Future work to investigate the effect of this volume fraction on the properties of the bioinspired materials is warranted, as this may open new opportunities for optimization.

Table 5.1 Dynamic testing results for samples from one (H-1) to six (H-6) levels of hierarchy, showing the density, normalized absorbed energy, flexural compliance and protecto-flexibility achieved by each sample configuration under impacts at 2ms-1. Changes in energy, flexural compliance and protecto-flexibility are compared with the H-1 samples.

Sample	 *H-1*	 *H-2*	 *H-4*	 *H-5H*	 *H-5R*	 *H-6*
Density (g/cm^3)	0.9	0.86	0.94	0.89	0.95	0.9
Normalized Energy (J/mm)	0.245	0.206	0.739	0.602	0.971	0.751
Change in Energy (%)	0%	-16%	202%	146%	297%	207%
Normalized Flexural Compliance (mm/kNmm)	2.102	2.515	3.053	4.041	2.527	3.878
Change in Flexural compliance (%)	0%	20%	45%	92%	20%	84%
Normalized Protecto-Flexibility (J/kN)	1.634	1.646	4.442	4.789	4.832	5.732
Change in Protecto-Flexibility (%)	0%	1%	172%	193%	196%	251%

The experimental results reveal that the different hierarchical structural levels analyzed here produce contrasting effects based on the specific configuration used. While superficial engravings increase flexibility and reduce protection, bioinspired nano-mineralization produces the opposite effect. Therefore, the protecto-flexibility metric is deemed to be the appropriate measure to the simultaneous contribution of protection and flexibility of the hierarchical bioinspired materials. Indeed, Figure 5.2b clearly shows that higher orders of hierarchy are associated with increased levels of protecto-flexibility, leading to a maximum increment of 251% in configurations reaching the highest orders of hierarchy, and with substantial similarities with biological analogs (*H-6*). Remarkably, this bioinspired configuration promotes a phenomenon that is present in segmented natural armor, where relatively stiffer mineralized units (separated by superficial engravings) can distribute localized loads over broader areas, while a flexible non-mineralized substrate provides flexibility, as shown schematically in Figure 5.4.

To further provide insight for future applications and designs we employed an analytical approach to predict the mechanical response of the bioinspired hierarchical materials. The model uses material's properties and relates them with geometrical parameters to predict the absorbed energy and flexural compliance of disc-shaped impact plates under the elastic regime of deformation (see Section 5.3). Model estimations are shown as circles in Figure 19 and are contrasted with the experimental results for both flexural compliance and normalized energy. These results show that model predictions are in good agreement with experimental data for *H-1, H-2, H-4* and *H-5H* samples, suggesting that the model can offer a good tool to estimate the mechanical effect of superficial engravings on monolithic and unreinforced laminated materials. However, for reinforced samples the model cannot accurately predict the experimental measurements. Specifically, the energy estimated by the model is below the energy levels reached by the experimental measurements for *H-5R* samples, supporting the idea that there are other mechanisms such as the increased interfacial friction between fibers responsible for increasing the mechanical performance of reinforced samples since this mechanism is not considered in the model in its present form. Nonetheless, these results suggest that bioinspiration can indeed guide the development of materials with apparently contradictory properties such as flexibility and protection.

To probe the concept proposed here, a bullet-proof vest insert was fabricated using the bioinspired configuration implemented in *H-6* samples (see Figure 17b), in which bioinspired mineralization, UHMWPE laminate structures, and engraving patterns were included. As shown in Figure 16a, engravings can offer high levels of flexibility according to their shape and orientation. Further, body armor designers could optimize the use of

engravings and bioinspired mineralization as schematically shown in Figure 17b. Consequently, engravings can be used in regions where flexibility is demanded, while mineralization is applied across the total surface of the armor insert, maximizing its protection capability. UHMWPE fiber arrangements are widely used by the armor industry in both soft and hard armor applications. (Attwood et al. 2015, 2016; Guo et al. 2017; Hani et al. 2012; Haque, Kearney, and Gillespie Jr. 2012; O'Masta et al. 2015; T. G. Zhang et al. 2015) However, while protection is optimized in hard armor, flexibility is maximized in soft armor with a considerable reduction in protection. Interestingly, the design shown in Figure 17b can optimize both flexibility and protection according to localized requirements: better protection in the chest and abdomen, with higher flexibility in the lateral regions where movements are expected. Aiming to validate this design, we conducted ballistic tests on the new protecto-flexible material (*H-6*). A 31 cm x 31 cm panel was impacted twice with 9 mm bullets at a distance of 5 m without any of the bullets penetrating through the bioinspired protecto-flexible material, as shown in Figure 16b and 17b. These remarkable results prove that the bioinspired materials can withstand ballistic impacts, and therefore show a promising route to enhance armor systems by using bioinspired methodologies. This exploration can guide the designs toward future protective systems, such as sports equipment and body armor.

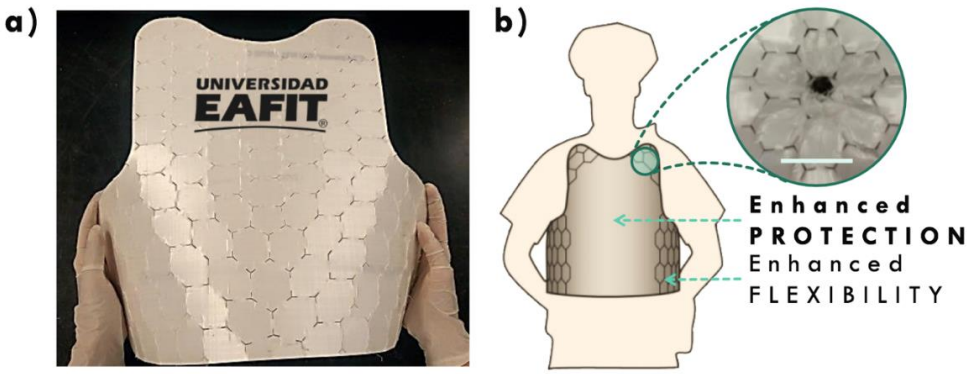

Figure 5.6 Ballistic application of bioinspired protecto-flexible materials. (a) Prototype of bullet proof insert for a protective vest showing how bioinspired engravings increase overall flexibility; (b) Scheme of bullet proof insert with optimized flexibility and protection according to localized requirements, the magnifying circle shows a 9 mm bullet impact on the bioinspired armor; scale bar corresponds to 50 mm.

One of the prime aims of this work was to develop hierarchical bioinspired cost-effective materials easily transferred to industry. The effect of the manufacturing process on protecto-flexibility of samples *H-4* to *H-6* can be analyzed if a figure of merit relating protecto-flexibility and density is compared with the added manufacturing costs, as shown in Figure 15. Note that increasing structural hierarchy to the samples improves their protecto-flexibility (up to ~30 %) with minimum associated manufacturing costs (< 3 %). Further, the manufacturing strategies proposed here can be easily implemented in high volumes of production, unlike bioinspired protection systems based on 3D printing technics. (Browning, Ortiz, and Boyce 2013; Gu, Takaffoli, and Buehler 2017; Jia, Yu, and Wang 2019; Martini, Balit, and Barthelat 2017; Rudykh, Ortiz, and Boyce 2015)

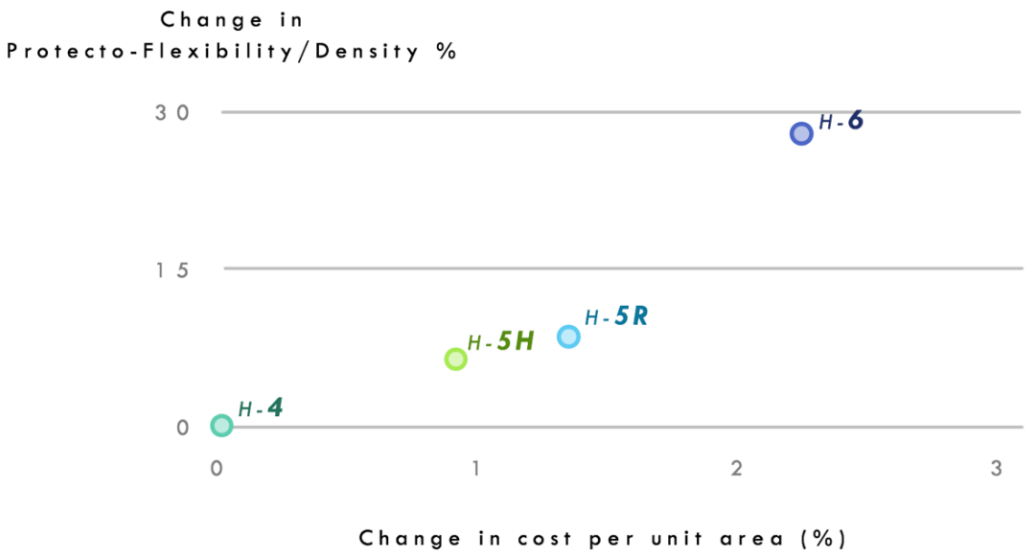

Figure 5.7 Change in material performance represented by protecto-flexibility and density as a function of the change in cost per unit area for the bioinspired materials H-4, H-5H, H-5R and H-6

5.3 Analytical model

As an initial guide to predict the mechanical response of the bioinspired hierarchical materials we use a simplified analytical model to estimate Load (P) and Absorbed Energy (U) under the linear elastic region of behavior of the material. Flexural Compliance (F_c) was used as a measure of flexibility. For a flat circular plate fixed by a clamping ring with a well-defined Radius (a) under a centered Load (P), Deflection (y) is described by (Michel 1901):

$$y = \frac{Pa^2}{16\pi\varsigma}. \tag{2}$$

The Energy (U) and Flexural compliance (F_c) can be written as:

$$U = \frac{yP}{2}, \tag{3}$$

and

$$F_c = \frac{y}{P}. \tag{4}$$

The term ς in Equation S1 corresponds to the plate constant, which is dependent on the thickness (t) of the plate, as well as mechanical properties of the material, such as Young's modulus (E) and Poisson's ratio (v). This constant (ς) is given by:

$$\varsigma = \frac{Et^3}{12(1-v^2)}. \tag{5}$$

For both mineralized and engraved samples, Young's Modulus (E) and Poisson's ratio (v) are estimated according to the manufacturing strategy used. For mineralized samples, E and v of the plate are estimated as a function of the Young's Modulus (E_m) and Poisson's ratio (v_m) of the matrix, and Young's Modulus (E_r), Poisson's ratio (v_r) and Volume fraction (V_f) of the reinforcement particles, following a rule of mixtures as:

$$E = E_m\left(1 - V_f\right) + E_r\left(V_f\right), \tag{6}$$

and

$$v = v_m\left(1 - V_f\right) + v_r(V_f)\,. \tag{7}$$

A similar strategy was followed to quantify E, v and plate thickness (t) of engraved plates as a function of Young's Modulus (E_u), Poisson's ratio (v_u) and thickness (t_u) of

unengraved plates and the volume of material removed from the laser engraving process (φ) as:

$$E = E_u(1-\varphi)\,, \tag{8}$$

$$v = v_u(1-\varphi)\,, \tag{9}$$

$$t = t_u(1-\varphi)\,. \tag{10}$$

φ is in turn estimated as a function of geometrical parameters like plate volume (ω), width (w) and depth (d) of engravings, the perimeter of the hexagons (s) and the number of hexagons (N) on the pattern, as:

$$\varphi = \frac{0.5wsdN}{\omega}. \tag{11}$$

Use of Equations 5-11 in Equations 2-4 makes possible to estimate the complete mechanical performance of the disk-shaped samples as a function of material properties and geometrical parameters. Specifically, Load (P), Absorbed Energy (U) and Flexural Compliance (F_c) as a function of Young's Modulus (E), and Poisson ratio (v) of the constitutive materials (considering whether the samples are mineralized or not), as well as geometrical parameters such as plate thickness (t), deflection (y), clamping ring radius (a), and volume fraction of material removed (φ) (if present), as:

$$P = \frac{4\pi y(E(1-\varphi))((t(1-\varphi))^3}{3a^2(1-(v(1-\varphi))^2))}, \tag{12}$$

$$U = \frac{3P^2a^2(1-(v(1-\varphi))^2)}{8\pi(E(1-\varphi))((t(1-\varphi))^3)}, \quad (13)$$

and

$$F_c = \frac{3a^2(1-(v(1-\varphi))^2)}{4\pi(E(1-\varphi))((t(1-\varphi))^3)}. \quad (14)$$

To compare the accuracy of the model predictions under the linear elastic region of behavior of the material, both absorbed energy (U) and flexural compliance (F_c) were calculated using Equations 13 and 14 and compared with experimental results for a deflection of 1mm (Figure 5.8). The modulus (E) used in the model was obtained experimentally through puncture tests ($E_{monolithic}$ =2.5 GPa and $E_{laminated}$ =11.3 GPa). Remarkably, for monolithic samples (*H-1* and *H-2*) and unreinforced laminates (*H-4* and *H-5*) the model prediction show a good accuracy when compared with experimental results, suggesting that volume fraction of material removed (φ) can in fact be used as an estimation of the mechanical effect of engraving on these kind of plates as a function of the geometrical parameters of engravings. On the other hand, the model accuracy for reinforced unengraved laminates (*H-5R*) is considered poor. The increase in absorbed energy is caused in this samples by an increment of the interfacial friction between fiber plies, and the model calculates this increment as a function of the volume fraction of the reinforcement particles (V_f), which is minimum (0.01). Finally, the model shows good accuracy with reinforced engraved laminates (*H-6)*, which could contradict the phenomenon observed in samples *H-5R* because both samples are nano-mineralized. However, this coincidence between model predictions and experimental measurements is caused by the discontinuity of mineralized fibers caused by superficial engravings, which

generates a similar behavior to that found in unreinforced engraved laminates (*H-5H*). Nevertheless, this similarity is only found at small deformation stages; at higher levels of deformation the differences between reinforced engraved (*H-6*) and unreinforced engraved (*H-5H*) samples is notable (see Figure 5.2b and 5.8). Future work using numerical modelling to study the effect of large deformations on the materials developed is warranted, as this may open new opportunities for optimization.

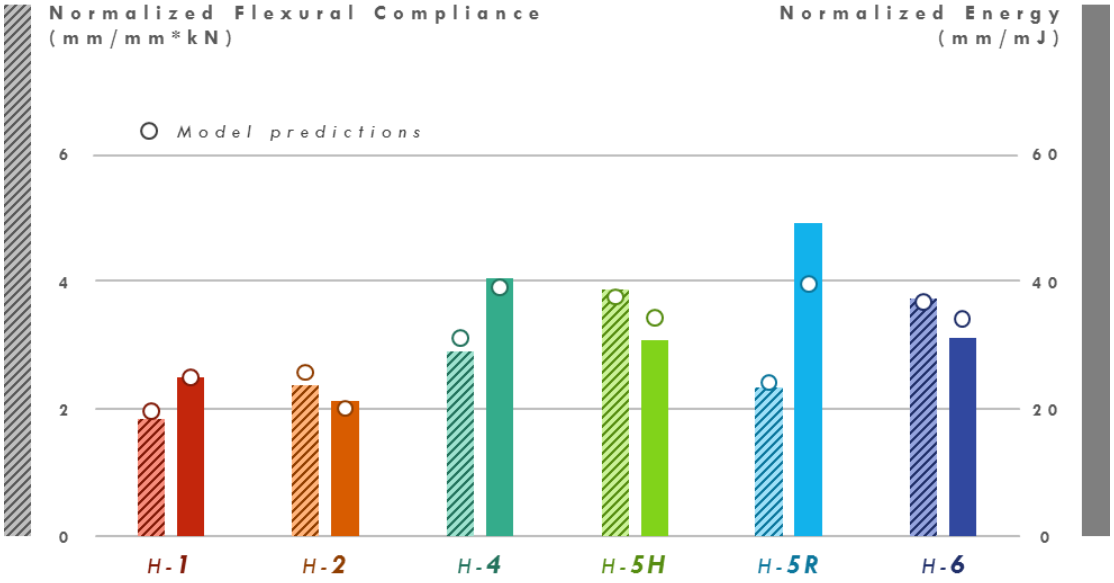

Figure 5.8 Measured levels of flexural compliance and normalized energy at a deflection of 1 mm. Stripped bars represent the measured flexural compliance corresponding to the left-hand axis; solid bars represent the measured normalized energy corresponding to the right-hand axis; model predictions are represented by circles.

5.4 Concluding remarks

Inspired by nature protection systems and its underlaying functional principles, a new family of protecto-flexible materials was developed. By using fish scales hierarchical structure and graded mineralization (to increase energy absorption and stiffness), and the

segmented patterns of armadillo's osteoderms (to increase flexibility), it was able to exploit the diverse energy absorbing mechanisms activated at different structural levels -from nano to macroscopic- to increase up to 251% the combined effect of energy absorption and flexibility on synthetic polymeric materials. Further, a bullet-proof protecto-flexible prototype was manufactured using the bioinspired principles investigated, finding that, under real stringent conditions, the novel system is capable of absorbing high levels of energy while being flexible enough to allow movement to the user. Remarkably, the material system developed allows its implementation into realistic high volumes of production with low added costs, so it is envisioned that the proposed strategy for developing bioinspired protecto-flexible materials will enable the development of the next generation of high-performance impact-resistant materials.

Chapter 6: Concluding remarks and main recommendations

6.1 Chapter 1

The search for impact-tolerant, light-weight flexible materials has challenged materials scientists in the last decades. In this quest, many researchers have focused on studying natural armors as a guide to propose bioinspired materials with enhanced properties. Due to its interdisciplinarity, bioinspired design causes translation difficulties between engineers and biologists. Therefore, this doctoral dissertation presents a simplified methodology for bioinspired design used to develop impact tolerant materials. By extracting the functional principles that underlay the extraordinary performance of segmented natural armor (i.e., segmentation, hierarchization, and graded mineralization), the resulting biomimetic materials exhibited a remarkable combination of properties including light-weight and enhanced protecto-flexibility. Due to the low added costs associated with the fabrication of these biomimetic materials, it is envisioned that they can encourage the development of the next generation of high-performance impact tolerant materials.

6.2 Chapter 2

Segmented natural armor is an extraordinary protective system found in different animal species including mammals, reptiles and fish. These arrangements are characterized by protecting against high predatory threats while enabling flexibility necessary for

locomotion. Despite their differences, these arrangements share common functional principles like segmentation, structural hierarchization and graded mineralization. By using biomimetics, some of these principles have inspired researchers in the last decades to develop extraordinary synthetic arrangements (e.g., laser engraved nacre-like arrangements, 3D printed scaled systems). However, while these studies help to establish the promise of bioinspired concepts in materials development, most of these concepts are far from industrial scalability due to their high added costs. Moreover, most of these approaches do not provide clear guidance to transfer the biological principles into synthetic industrially scalable configurations. Therefore, new methods and tools are necessary to provide clear guidance in bioinspired design processes.

6.3 Chapter 3

After millions of years of evolution, natural systems have inspired engineers to design and fabricate novel materials and devices with enhanced attributes and properties. This discipline is known as biomimetics and is characterized by moving across two different domains of knowledge: biology and engineering. This multidisciplinary nature is a fertile scenario for the emergence of novel design concepts. However, language differences between engineers and biologists generate implementation difficulties for bioinspired design. Aiming to close the gap between these two domains of knowledge, multiple design methodologies for bioinspired design has emerged in the last decades, however, most of them are hardly implemented in industrial scenarios due to their complex and overwhelming routes.

This work proposes that instead of using complex methodologies, simplification is key for biomimetics popularization. Current successful bioinspired developments such as Velcro and Fastskin support that idea. Consequently, this work proposed a simplified methodology for bioinspired design comprised of the following four steps:

1) Define.
2) Search.
3) Simplify.
4) Conceptualize.

To test the proposed methodology in a real design challenge, the methodology was used to develop bioinspired design concepts for flexible protection obtaining simple ideas that can be replicated using current manufacturing technics. On one hand, laser engraving was proposed to introduce superficial segmentation within synthetic materials aiming to obtain enhanced flexibility. On the other hand, the use of laminar composites was proposed to introduce new levels of hierarchy in synthetic arrangements. Finally, by using the proposed simplified methodology, a novel manufacturing process emerged: bioinspired nano-mineralization. This new technic allows mimicking the graded mineralization present in fish scales.

6.4 Chapter 4

By using a novel fabrication strategy called bioinspired nano mineralization it was able to mimic the graded mineralization exhibited by Arapaima scales, with a variation in the mineral content from the top to the bottom of the material. By using two different nano mineralization strategies (i.e., Al_2O_3 nanoparticles and TiN nanocoating) into a laminar

organic fibrous composite, three different sample typologies were obtained: *i)* unreinforced, *ii)* reinforced with Al_2O_3, and *iii)* reinforced with TiN. Dynamic tests revealed that the impact resistance of the reinforced materials was increased significantly with respect to the non-reinforced materials, with a 20% to 23% increase in absorbed energy for materials reinforced with Al_2O_3 and TiN respectively. Remarkably, this enhancement in impact performance was obtained with a negligible increase in the weight (i.e., less than 2,5 % in Al_2O_3-reinfoced materials and barely 0,15 % in TiN-reinforced materials). The microscopy analysis suggested that the enhanced impact performance resulted from a new energy dissipation mechanism at the nanoscale. This mechanism involves increased friction between the fibrous layers of the laminate through interfacial nano-scale reinforcements. Remarkably, the Al_2O_3-based mineralization strategy can be industrially scaled up due to their low added costs. Therefore, this strategy for developing bioinspired hierarchical materials may bring the benefits of biomimetics to the next generation of light-weight, cost-efficient, impact-tolerant, high-performance protective materials.

6.5 Chapter 5

Inspired by nature protection systems and its underlaying functional principles, a new family of protecto-flexible materials was developed. By using fish scales hierarchical structure and graded mineralization (to increase energy absorption and stiffness), and the segmented patterns of armadillo's osteoderms (to increase flexibility), it was able to exploit the diverse energy absorbing mechanisms activated at different structural levels -from nano to macroscopic- to increase up to 251% the combined effect of energy absorption and flexibility on synthetic polymeric materials. Further, a bullet-proof protecto-flexible

prototype was manufactured using the bioinspired principles investigated, finding that, under real stringent conditions, the novel system is capable of absorbing high levels of energy while being flexible enough to allow movement to the user. Remarkably, the material system developed allows its implementation into realistic high volumes of production with low added costs, so it is envisioned that the proposed strategy for developing bioinspired protecto-flexible materials will enable the development of the next generation of high-performance impact-resistant materials.

6.6 Main recommendations

First, a little patience is helpful when dealing with bioinspired design challenges. Although the results here are presented as a well-organized linear succession of events, real design processes are complex and iterative.

Regarding bioinspired nano mineralization, and specifically to mineralization based on nanoparticles, it would be recommended to investigate the mechanical effect of varying the size of the nanoparticles. As the interplay between fibers and nanoparticles have proven to affect the mechanical performance of organic fibrous laminar composites, changes in particle size would presumably affect this interplay, thus promoting different consequences in the laminate behavior. The Al_2O_3 nanoparticles used here exhibited an average diameter of 500nm, however, multiple nanoparticle sizes are commercially available. By varying particle sizes new opportunities for optimization can be opened. Likewise, the bioinspired nano mineralized composites can be also modified to achieve a mineral gradient closer to that found in fish scales. This is, instead of using a fixed volume fraction of nanoparticles in the most external layers of the bioinspired materials, graded volume fractions can be

used maintaining a stacking sequence in which layers covered with higher degrees of mineral volume fraction are sequentially organized towards the outermost surface of the laminate (see Figure 6.1).

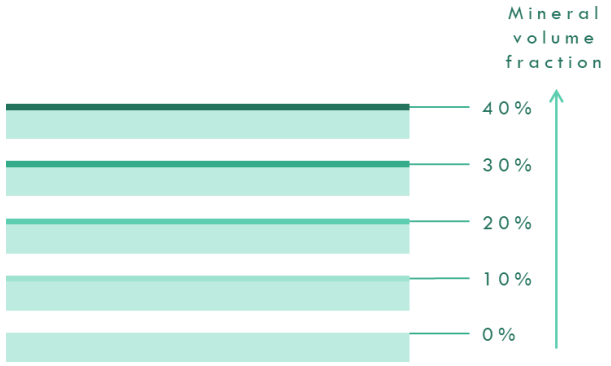

Figure 6.1Example of bioinspired nano mineralization with differences in the mineral content present in the organic layers.

Regarding segmentation, it would be recommended to investigate the mechanical consequences of using geometrical patterns with varying edge length. Moreover, the geometrical pattern itself can also be investigated by varying its basic repetitive shape. This is, compare the performance differences between materials engraved with hexagons, squares and triangles. These studies may also suggest new opportunities for optimization.

Finally, by simultaneously exploiting different biological functional principles in synthetic materials, it was possible to achieve typically mutually exclusive properties in synthetic materials. This suggests that the combined effect of multiple functional principles may lead to extraordinary properties, and thus, the identification of different functional principles in bioinspired design processes is encouraged.

References

Allison, P. G. et al. 2013. "Mechanical Properties and Structure of the Biological Multilayered Material System, Atractosteus Spatula Scales." *Acta Biomaterialia* 9(2): 5289–96.

Arola, D. et al. 2018. "The Limiting Layer of Fish Scales: Structure and Properties." *Acta Biomaterialia* 67: 319–30.

Askarinejad, Sina, and Nima Rahbar. 2018. "Mechanics of Bioinspired Lamellar Structured Ceramic/Polymer Composites: Experiments and Models." *International Journal of Plasticity* 107(April): 122–49.

Attwood, J. P., N. A. Fleck, H. N G Wadley, and V. S. Deshpande. 2015. "The Compressive Response of Ultra-High Molecular Weight Polyethylene Fibres and Composites." *International Journal of Solids and Structures* 71: 141–55.

Attwood, J. P., B.P. Russel, H.N.G Wadley, and V.S. Deshpande. 2016. "Mechanisms of the Penetration of Ultra-High Molecular Weight Polyethylene Composite Beams." *International Journal of Impact Engineering* 93: 153–65.

Bar-Cohen, Yoseph. 2006. "Biomimetics - Using Nature to Inspire Human Innovation." *Bioinspiration and Biomimetics* 1(1): 1–12.

Barthelat, F. 2015. "Architectured Materials in Engineering and Biology: Fabrication, Structure, Mechanics and Performance." *International Materials Reviews* 60(8): 413–30.

Barthelat, F, and D J Zhu. 2011. "A Novel Biomimetic Material Duplicating the Structure and Mechanics of Natural Nacre." *Journal of Materials Research* 26(10): 1203–15.

Barthelat, Francois. 2007. "Biomimetics for next Generation Materials." *Philosophical Transactions of the Royal Society A: Mathematical, Physical and Engineering Sciences* 365(1861): 2907–19.

Bhushan, Bharat. 2009. "Biomimetics: Lessons from Nature - an Overview." *Philosophical Transactions of the Royal Society A: Mathematical, Physical and Engineering Sciences* 367(1893): 1445–86.

Browning, Ashley, Christine Ortiz, and Mary C Boyce. 2013. "Mechanics of Composite Elasmoid Fish Scale Assemblies and Their Bioinspired Analogues." *Journal of the mechanical behavior of*

biomedical materials 19: 75–86.

Bruet, Benjamin J.F., Juha Song, Mary C. Boyce, and Christine Ortiz. 2008. "Materials Design Principles of Ancient Fish Armour." *Nature Materials* 7(9): 748–56.

Burghard, Zaklina et al. 2009. "Toughening through Natu Re-Adapted Nanoscale Design." *Nano Letters* 9(12): 4103–8.

Chen, Irene H. et al. 2011. "Armadillo Armor: Mechanical Testing and Micro-Structural Evaluation." *Journal of the Mechanical Behavior of Biomedical Materials* 4(5): 713–22. http://dx.doi.org/10.1016/j.jmbbm.2010.12.013.

Chen, Irene H., Wen Yang, and Marc A. Meyers. 2014. "Alligator Osteoderms: Mechanical Behavior and Hierarchical Structure." *Materials Science and Engineering C* 35(1): 441–48. http://dx.doi.org/10.1016/j.msec.2013.11.024.

———. 2015. "Leatherback Sea Turtle Shell: A Tough and Flexible Biological Design." *Acta Biomaterialia* 28(SEPTEMBER): 2–12.

Cheong, H. et al. 2011. "Biologically Meaningful Keywords for Functional Terms of the Functional Basis." *Journal of Mechanical Design, Transactions of the ASME* 133(2): 1–11.

Chintapalli, Ravi Kiran, Mohammad Mirkhalaf, Ahmad Khayer Dastjerdi, and Francois Barthelat. 2014. "Fabrication, Testing and Modeling of a New Flexible Armor Inspired from Natural Fish Scales and Osteoderms." *Bioinspiration & Biomimetics* 9(3): 036005. https://iopscience.iop.org/article/10.1088/1748-3182/9/3/036005.

Crouch, Ian G. 2019. "Body Armour – New Materials, New Systems." *Defence Technology* 15(3): 241–53.

Damiens, R et al. 2012. "Compressive Behavior of a Turtle's Shell: Experiment, Modeling, and Simulation." *Journal of the mechanical behavior of biomedical materials* 6: 106–12.

Dastjerdi, Ahmad Khayer, Reza Rabiei, and Francois Barthelat. 2013. "The Weak Interfaces within Tough Natural Composites: Experiments on Three Types of Nacre." *Journal of the Mechanical Behavior of Biomedical Materials* 19: 50–60. http://dx.doi.org/10.1016/j.jmbbm.2012.09.004.

Ding, Jie et al. 2013. "Review on Shear Thickening Fluids and Applications." *Textiles and Light Industrial Science and Technology* 2(4): 161–73.

DiPette, Scott, Ani Ural, and Sridhar Santhanam. 2015. "Analysis of Toughening Mechanisms in the Strombus Gigas Shell." *Journal of the Mechanical Behavior of Biomedical Materials* 48: 200–209.

Duro-Royo, Jorge et al. 2015. "MetaMesh: A Hierarchical Computational Model for Design and Fabrication of Biomimetic Armored Surfaces." *CAD Computer Aided Design* 60: 14–27. http://dx.doi.org/10.1016/j.cad.2014.05.005.

Eidini, Maryam. 2016. "Zigzag-Base Folded Sheet Cellular Mechanical Metamaterials." *Extreme Mechanics Letters* 6: 96–102.

Fayemi, P. E. et al. 2017. "Biomimetics: Process, Tools and Practice." *Bioinspiration and Biomimetics* 12(1).

Gao, Chao, and Yaning Li. 2019. "Mechanical Model of Bio-Inspired Composites with Sutural Tessellation." *Journal of the Mechanics and Physics of Solids* 122: 190–204. https://doi.org/10.1016/j.jmps.2018.09.015.

Ghods, S., S. Murcia, E. A. Ossa, and D. Arola. 2019. "Designed for Resistance to Puncture: The Dynamic Response of Fish Scales." *Journal of the Mechanical Behavior of Biomedical Materials* 90(May 2018): 451–59.

Glier, Michael W., Daniel A. McAdams, and Julie S. Linsey. 2011. "Concepts in Biomimetic Design: Methods and Tools to Incorporate into a Biomimetic Design Course." In *Proceedings of the ASME Design Engineering Technical Conference*, , 655–60.

Grunenfelder, L. K. et al. 2014. "Bio-Inspired Impact-Resistant Composites." *Acta Biomaterialia* 10(9): 3997–4008.

Gu, Grace X., Mahdi Takaffoli, and Markus J. Buehler. 2017. "Hierarchically Enhanced Impact Resistance of Bioinspired Composites." *Advanced Materials* 29(28): 1700060. http://doi.wiley.com/10.1002/adma.201700060.

Guo, Zherui et al. 2017. "Multi-Scale Experiments on Soft Body Armors under Projectile Normal Impact." *Proceedings - 30th International Symposium on Ballistics, BALLISTICS 2017* 2: 1935–46.

Gürgen, Selim, Melih Cemal Kuşhan, and Weihua Li. 2017. "Shear Thickening Fluids in Protective Applications: A Review." *Progress in Polymer Science* 75: 48–72.

Han, Zhiwu et al. 2016. "Biomimetic Multifunctional Surfaces Inspired from Animals." *Advances in Colloid and Interface Science* 234: 27–50. http://dx.doi.org/10.1016/j.cis.2016.03.004.

Hani, A.R. Azrin, A. Roslan, J. Mariatti, and M. Maziah. 2012. "Body Armor Technology: A Review of Materials, Construction Techniques and Enhancement of Ballistic Energy Absorption." *Advanced Materials Research* 488–489: 806–12.

Haque, B Z, M M Kearney, and J W Gillespie Jr. 2012. "Advances in Protective Personnel and Vehicle Armors." *Recent Patents on Materials Science* 5(2): 105–36.

Hazzard, Mark K. et al. 2017. "Effect of Fibre Orientation on the Low Velocity Impact Response of Thin Dyneema® Composite Laminates." *International Journal of Impact Engineering* 100: 35–45.

Helms, Michael E. et al. 2008. "Problem-Driven and Solution-Based Design Twin Processes of Biologically Inspired Design." *ACADIA 08: Silicon + Skin: Biological Processes and Computation: Proceedings of the 28th Annual Conference of the Association for Computer Aided Design in Architecture*: 94–99.

Helms, Michael, and Ashok K. Goel. 2014. "The Four-Box Method: Problem Formulation and Analogy Evaluation in Biologically Inspired Design." *Journal of Mechanical Design, Transactions of the ASME* 136(11).

Helms, Michael, Swaroop S. Vattam, and Ashok K. Goel. 2009. "Biologically Inspired Design: Process and Products." *Design Studies* 30(5): 606–22. http://dx.doi.org/10.1016/j.destud.2009.04.003.

Huang, Wei et al. 2019. "Multiscale Toughening Mechanisms in Biological Materials and Bioinspired Designs." *Advanced Materials* 1901561: 1901561.

Jayasankar, A. K. et al. 2017. "Mechanical Behavior of Idealized, Stingray-Skeleton-Inspired Tiled Composites as a Function of Geometry and Material Properties." *Journal of the Mechanical Behavior of Biomedical Materials* 73(August 2016): 86–101. http://dx.doi.org/10.1016/j.jmbbm.2017.02.028.

Jia, Zian, Yang Yu, and Lifeng Wang. 2019. "Learning from Nature: Use Material Architecture to Break the Performance Tradeoffs." *Materials & Design* 168: 107650. https://linkinghub.elsevier.com/retrieve/pii/S0264127519300875.

Jiang, H. et al. 2020. "Contributions of Intermolecular Bonding and Lubrication to the Mechanical Behavior of a Natural Armor." *Acta Biomaterialia* (xxxx).

Kardong, Kenneth V. 2012. *Vertebrates Comparative Anatomy, Function, Evolution*. 6th ed. Mc Graw Hill.

Khayer Dastjerdi, A., and F. Barthelat. 2015. "Teleost Fish Scales amongst the Toughest Collagenous Materials." *Journal of the Mechanical Behavior of Biomedical Materials* 52: 95–107.

Lenau, T., A. Dentel, P. Ingvarsdóttir, and T. Guolaugsson. 2010. "Engineering Design of an Adaptive Leg Prosthesis Using Biological Principles." In *11th International Design Conference, DESIGN 2010*, , 331–40.

Lenau, Torben. 2009. "Biomimetics as a Design Methodology - Possibilities and Challenges." In *Internation Conference on Engineering Design, ICED'09*, Stanford, 121–32.

Lenau, Torben Anker, Sonal Keshwani, Amaresh Chakrabarti, and Saeema Ahmed-Kristensen. 2015. "Biocards and Level of Abstraction." *Proceedings of the International Conference on Engineering Design, ICED* 2(DS 80-02): 177–86.

Lepora, Nathan F., Paul Verschure, and Tony J. Prescott. 2013. "The State of the Art in Biomimetics." *Bioinspiration and Biomimetics* 8(1).

Li, Zan et al. 2015. "Enhanced Mechanical Properties of Graphene (Reduced Graphene Oxide)/Aluminum Composites with a Bioinspired Nanolaminated Structure." *Nano Letters* 15(12): 8077–83.

Lin, Y. S., C. T. Wei, E. A. Olevsky, and Marc A. Meyers. 2011. "Mechanical Properties and the Laminate Structure of Arapaima Gigas Scales." *Journal of the Mechanical Behavior of Biomedical Materials* 4(7): 1145–56.

Lindemann, U., and J. Gramann. 2004. "Engineering Design Using Biological Principles." *Proceedings of DESIGN 2004, the 8th International Design Conference, Dubrovnik, Croatia*: 355–60. https://www.designsociety.org/publication/19775/ENGINEERING+DESIGN+USING+BIOLOGICAL+PRINCIPLES.

Liu, Z. Q., D. Jiao, Z. Y. Weng, and Z. F. Zhang. 2016. "Structure and Mechanical Behaviors of Protective Armored Pangolin Scales and Effects of Hydration and Orientation." *Journal of the Mechanical Behavior of Biomedical Materials* 56: 165–74.

López, Marlén, Ramón Rubio, Santiago Martín, and Ben Croxford. 2017. "How Plants Inspire Façades. From Plants to Architecture: Biomimetic Principles for the Development of Adaptive Architectural

Envelopes." *Renewable and Sustainable Energy Reviews* 67: 692–703. http://dx.doi.org/10.1016/j.rser.2016.09.018.

Martini, R., Y. Balit, and F. Barthelat. 2017. "A Comparative Study of Bio-Inspired Protective Scales Using 3D Printing and Mechanical Testing." *Acta Biomaterialia* 55: 360–72.

Martini, R., and F. Barthelat. 2016a. "Stability of Hard Plates on Soft Substrates and Application to the Design of Bioinspired Segmented Armor." *Journal of the Mechanics and Physics of Solids* 92: 195–209.

Martini, R, and F Barthelat. 2016b. "Stretch-and-Release Fabrication, Testing and Optimization of a Flexible Ceramic Armor Inspired from Fish Scales." *Bioinspiration & biomimetics* 11.

Meyers, M. A., Y. S. Lin, E. A. Olevsky, and P.-Y. Chen. 2012. "Battle in the Amazon: Arapaima versus Piranha." *Advanced Engineering Materials* 14(5): B279–88.

Meyers, Marc A. et al. 2011. "Biological Materials: A Materials Science Approach." *Journal of the Mechanical Behavior of Biomedical Materials* 4(5): 626–57.

Meyers, Marc André, Po Yu Chen, Albert Yu Min Lin, and Yasuaki Seki. 2008. "Biological Materials: Structure and Mechanical Properties." *Progress in Materials Science* 53(1): 1–206.

Miao, Tingyi et al. 2019. "Ballistic Performance of Bioinspired Nacre-like Aluminium Composite Plates." *Composites Part B: Engineering* 177(August).

Michel, J. H. 1901. "The Flexure of a Circular Plate." *Proceedings of the London Mathematical Society* s1-34(1): 223–34.

Mirkhalaf, M., J. Tanguay, and F. Barthelat. 2016. "Carving 3D Architectures within Glass: Exploring New Strategies to Transform the Mechanics and Performance of Materials." *Extreme Mechanics Letters* 7: 104–13.

Murcia, Sandra et al. 2015. "Temperature Effects on the Fracture Resistance of Scales from Cyprinus Carpio." *Acta Biomaterialia* 14: 154–63. http://dx.doi.org/10.1016/j.actbio.2014.11.034.

———. 2016. "Effects of Polar Solvents on the Mechanical Behavior of Fish Scales." *Materials Science and Engineering C* 61: 23–31.

———. 2017. "The Natural Armors of Fish: A Comparison of the Lamination Pattern and Structure of

Scales." *Journal of the Mechanical Behavior of Biomedical Materials* 73(September 2016): 17–27.

Nagel, Jacquelyn K.S., Robert L. Nagel, Robert B. Stone, and Daniel A. McAdams. 2010. "Function-Based, Biologically Inspired Concept Generation." *Artificial Intelligence for Engineering Design, Analysis and Manufacturing: AIEDAM* 24(4): 521–35.

O'Masta, M. R., D. H. Crayton, V. S. Deshpande, and H. N G Wadley. 2015. "Mechanisms of Penetration in Polyethylene Reinforced Cross-Ply Laminates." *International Journal of Impact Engineering* 86: 249–64.

Radwan, Gehan.A.N., and Nouran Osama. 2016. "Biomimicry, an Approach, for Energy Effecient Building Skin Design." *Procedia Environmental Sciences* 34: 178–89. http://dx.doi.org/10.1016/j.proenv.2016.04.017.

Rafsanjani, Ahmad, and Damiano Pasini. 2016. "Bistable Auxetic Mechanical Metamaterials Inspired by Ancient Geometric Motifs." *Extreme Mechanics Letters* 9: 291–96.

Reis, Pedro M., Heinrich M. Jaeger, and Martin van Hecke. 2015. "Designer Matter: A Perspective." *Extreme Mechanics Letters* 5: 25–29.

Rudykh, Stephan, Christine Ortiz, and Mary C. Boyce. 2015. "Flexibility and Protection by Design: Imbricated Hybrid Microstructures of Bio-Inspired Armor." *Soft Matter* 11(13): 2547–54.

Sabu, Chinnu, Christine Rejo, Sabna Kotta, and K. Pramod. 2018. "Bioinspired and Biomimetic Systems for Advanced Drug and Gene Delivery." *Journal of Controlled Release* 287(August): 142–55. https://doi.org/10.1016/j.jconrel.2018.08.033.

Shan, Sicong et al. 2015. "Design of Planar Isotropic Negative Poisson's Ratio Structures." *Extreme Mechanics Letters* 4: 96–102.

Sherman, Vincent R. et al. 2017. "A Comparative Study of Piscine Defense: The Scales of Arapaima Gigas, Latimeria Chalumnae and Atractosteus Spatula." *Journal of the Mechanical Behavior of Biomedical Materials* 73(October 2016): 1–16.

Shu, L. H., K. Ueda, I. Chiu, and H. Cheong. 2011. "Biologically Inspired Design." *CIRP Annals - Manufacturing Technology* 60(2): 673–93. http://dx.doi.org/10.1016/j.cirp.2011.06.001.

Sire, Jean Yves, and Ann Huysseune. 2003. "Formation of Dermal Skeletal and Dental Tissues in Fish: A

Comparative and Evolutionary Approach." *Biological Reviews of the Cambridge Philosophical Society* 78(2): 219–49.

Song, Ningning, Yunya Zhang, Zan Gao, and Xiaodong Li. 2018. "Bioinspired, Multiscale Reinforced Composites with Exceptionally High Strength and Toughness." *Nano Letters* 18(9): 5812–20.

Suksangpanya, Nobphadon, Nicholas A. Yaraghi, David Kisailus, and Pablo Zavattieri. 2017. "Twisting Cracks in Bouligand Structures." *Journal of the Mechanical Behavior of Biomedical Materials* 76(March): 38–57.

Sun, Chang-Yu Yu, and Po-Yu Yu Chen. 2013. "Structural Design and Mechanical Behavior of Alligator (Alligator Mississippiensis) Osteoderms." *Acta biomaterialia* 9(11): 9049–64.

Sun, Liang Liang, Dang Sheng Xiong, and Cai Yun Xu. 2013. "Application of Shear Thickening Fluid in Ultra High Molecular Weight Polyethylene Fabric." *Journal of Applied Polymer Science* 129(4): 1922–28.

Tsang, H. H., and S. Raza. 2018. "Impact Energy Absorption of Bio-Inspired Tubular Sections with Structural Hierarchy." *Composite Structures* 195(April): 199–210.

Valashani, Seyed Mohammad Mirkhalaf, and Francois Barthelat. 2015. "A Laser-Engraved Glass Duplicating the Structure, Mechanics and Performance of Natural Nacre." *Bioinspiration & Biomimetics* 10(2): 026005. https://iopscience.iop.org/article/10.1088/1748-3190/10/2/026005.

Vernerey, Franck J., and Francois Barthelat. 2010. "On the Mechanics of Fishscale Structures." *International Journal of Solids and Structures* 47(17): 2268–75.

Vincent, Julian F.V. et al. 2006. "Biomimetics: Its Practice and Theory." *Journal of the Royal Society Interface* 3(9): 471–82.

Volstad, Nina Louise, and Casper Boks. 2012. "On the Use of Biomimicry as a Useful Tool for the Industrial Designer." *Sustainable Development* 20(3): 189–99.

Wang, Bin, Wen Yang, Vincent R. Sherman, and Marc A. Meyers. 2016. "Pangolin Armor: Overlapping, Structure, and Mechanical Properties of the Keratinous Scales." *Acta Biomaterialia* 41(May): 60–74.

Wanieck, Kristina et al. 2016. "Biomimetics and Its Tools." *Bioinspired, Biomimetic and Nanobiomaterials* 6(2): 53–66.

Yang, Wen, Irene H. Chen, et al. 2013. "Natural Flexible Dermal Armor." *Advanced Materials* 25(1): 31–48.

Yang, Wen, Bernd Gludovatz, et al. 2013. "Structure and Fracture Resistance of Alligator Gar (Atractosteus Spatula) Armored Fish Scales." *Acta Biomaterialia* 9(4): 5876–89.

Yang, Wen et al. 2014. "Protective Role of Arapaima Gigas Fish Scales: Structure and Mechanical Behavior." *Acta Biomaterialia* 10(8): 3599–3614. http://dx.doi.org/10.1016/j.actbio.2014.04.009.

Yang, Wen, Irene H. Chen, Joanna Mckittrick, and Marc a. Meyers. 2012. "Flexible Dermal Armor in Nature." *JOM* 64(4): 475–85. http://link.springer.com/10.1007/s11837-012-0301-9.

Yang, Wen, Marc A. Meyers, and Robert O. Ritchie. 2019. "Structural Architectures with Toughening Mechanisms in Nature: A Review of the Materials Science of Type-I Collagenous Materials." *Progress in Materials Science* 103(January): 425–83.

Yang, Wen, Haocheng Quan, Marc A. Meyers, and Robert O. Ritchie. 2019a. "Arapaima Fish Scale: One of the Toughest Flexible Biological Materials." *Matter*: 1–10. https://doi.org/10.1016/j.matt.2019.09.014.

———. 2019b. "Arapaima Fish Scale: One of the Toughest Flexible Biological Materials." *Matter* 1: 1–10.

Yin, Z, F Hannard, and F Barthelat. 2019. "Impact-Resistant Nacre-like Transparent Materials." *Science* 364(6447): 1260–63.

Yin, Zhen, Ahmad Dastjerdi, and Francois Barthelat. 2018. "Tough and Deformable Glasses with Bioinspired Cross-Ply Architectures." *Acta Biomaterialia* 75: 439–50.

Zhang, Timothy G., Sikhanda S. Satapathy, Lionel R. Vargas-Gonzalez, and Shawn M. Walsh. 2015. "Ballistic Impact Response of Ultra-High-Molecular-Weight Polyethylene (UHMWPE)." *Composite Structures* 133: 191–201.

Zhang, Xu, Zhen bing Cai, Wei Li, and Min hao Zhu. 2018. "Understanding Hydration Effects on Mechanical and Impacting Properties of Turtle Shell." *Journal of the Mechanical Behavior of Biomedical Materials* 78(June 2017): 116–23.

Zhang, Yunya, and Xiaodong Li. 2017. "Bioinspired, Graphene/Al 2 O 3 Doubly Reinforced Aluminum Composites with High Strength and Toughness." *Nano Letters* 17(11): 6907–15.

Zhou, Fei, Zhiwei Wu, Meiling Wang, and Kangmin Chen. 2010. "Structure and Mechanical Properties of Pincers of Lobster (Procambarus Clarkii) and Crab (Eriocheir Sinensis)." *Journal of the Mechanical Behavior of Biomedical Materials* 3(6): 454–63.

Zhu, Deju et al. 2012. "Structure and Mechanical Performance of a 'Modern' Fish Scale." *Advanced Engineering Materials* 14(4).

Zhu, Deju, Lawrence Szewciw, Franck Vernerey, and Francois Barthelat. 2013. "Puncture Resistance of the Scaled Skin from Striped Bass: Collective Mechanisms and Inspiration for New Flexible Armor Designs." *Journal of the mechanical behavior of biomedical materials* 24: 30–40.

Zimmermann, Elizabeth A. et al. 2013. "Mechanical Adaptability of the Bouligand-Type Structure in Natural Dermal Armour." *Nature Communications* 4(October): 1–7.

Zuazua-Ros, Amaia, César Martín-Gómez, Juan Carlos Ramos, and Tomás Gómez-Acebo. 2017. "Bio-Inspired Heat Dissipation System Integrated in Buildings: Development and Applications." *Energy Procedia* 111(September 2016): 51–60. http://dx.doi.org/10.1016/j.egypro.2017.03.007.